Current Research in Food Science 9 (2024) 100923

Contents lists available at ScienceDirect

Current Research in Food Science

journal homepage: www.sciencedirect.com/journal/current-research-in-food-science

Optimization of cold-induced aerated gels formed by Maillard-driven conjugates of SPI-gellan gum as an oil substitute in mayonnaise sauce

Setayesh Ferdowsian, Zahra Kazemi-Taskooh, Mohammad Javad Varidi *, Majid Nooshkam, Mehdi Varidi **

Department of Food Science and Technology, Faculty of Agriculture, Ferdowsi University of Mashhad, Azadi Sq., Mashhad, Khorasan Razavi, P.O. Box 9177948944, Iran

ARTICLE INFO

Keywords:
Binary gels
Grafting
Maillard reaction
Oil substitute
Plant-based product
RSM

ABSTRACT

This research aimed at characterization of composite cold-set aerated gels composed of SPI-gellan gum Maillard conjugates. The optimized gel was eventually incorporated in mayonnaise sauce as an oil substitute. The optimum conditions were statistically determined as 1.5% SPI, 300 mM $CaCl_2$, and 90 min heating time. All of which resulted 35% glycation degree and high molecular weight conjugates on top of SDS-PAGE injection wells. Increasing $CaCl_2$ concentration enhanced the adsorption of conjugates at air-water interface, decreasing the density but increasing the WHC and hardness. Increasing heating time facilitated gelation which improved gel hardness. The optimized gel was microstructurally homogeneous with increased overrun (20.8%) and H-bonds. The rheological measurements showed viscoelastic gel network which was thermally stable up to 90 °C, besides increasing G', G" and η* at 85 °C. Substitution of optimized gel in mayonnaise sauce improved the nutritional value and thermal stability (77.13%), but declined calorie. The substituted mayonnaise sauce was greatly accepted by panelists. Thus, the aerated gel formed at optimum conditions had great structural and mechanical characteristics and its usage as an oil analogue induced a low-calorie mayonnaise sauce with acceptable sensory properties.

1. Introduction

Mayonnaise is an oil-in-water emulsion, containing two immiscible or partially miscible components (Pourramezan et al., 2022). The common mayonnaise sauces contain at least 65% oil which may cause obesity and cardiovascular diseases. The consumers' tendency toward low-calorie products have increased the demand for low fat foodstuffs. However, reduced-fat foodstuffs struggle with decreased organoleptic and mechanical properties, so the development of a product with a comparable sensory profile sounds challenging (X. Yang et al., 2020). The bigels from cold-pressed chia seed oil (Alkabaa et al., 2024) and fish oil (Sun et al., 2025), and the oleogels of sesame oil (Gharachorloo and Yousefi, 2024) were previously substituted with the oil of mayonnaise. All of which were structuralized oils for reducing trans- and saturated-fatty acids (Sun et al., 2025), while aerated gel with a non-oily structure was not yet used to produce low-calorie mayonnaise sauce.

Recent years have seen renewed interest in aerated structures since they facilitate the food digestion besides reducing food calorie and inducing satiety (Zúñiga and Aguilera, 2008). Aerated gels, considered as biphasic colloidal systems, entrap gas bubbles in a semi-solid structure (Pourramezan et al., 2022). The structures containing air bubbles provide vast interfaces which increases the free energy, causing the network thermodynamically unstable. So, surface active agents are required to reduce the surface tension by decreasing the free energy, stabilizing the aerated gels (Deng et al., 2019). Protein-based aerated gels have been previously characterized (Tomczyńska-Mleko et al., 2022). It was shown that proteins can stabilize the air bubbles as surface actives (Zúñiga and Aguilera, 2008).

Plant-derived proteins have recently attracted vast attention thanks to the dietary preferences of consumers in terms of eco- and animal-friendly concerns, lower cost, and cultural concerns. Moreover, plant-based proteins containing well-balanced amino acids exhibit higher

* Corresponding author.
** Corresponding author.
E-mail addresses: Frdsetayesh@gmail.com (S. Ferdowsian), Kazemitaskooh.zahra@mail.um.ac.ir (Z. Kazemi-Taskooh), Mjvaridi@um.ac.ir (M.J. Varidi), Nooshkamma@gmail.com (M. Nooshkam), M.varidi@um.ac.ir (M. Varidi).

https://doi.org/10.1016/j.crfs.2024.100923
Received 13 September 2024; Received in revised form 27 October 2024; Accepted 9 November 2024
Available online 10 November 2024

sustainability compared with animal ones (Abaee et al., 2017). To the best of our knowledge, soy protein-based aerated gel was not yet characterized. However, soy proteins possess a compact globular tertiary structure high molecular weight which reduces protein solubility, resulting in restricted foaming capacity (Ma et al., 2020). Hence, soy proteins show undesirable surface activity (Abaee et al., 2017), demanding modifications.

Various methods can be applied to modify the proteins' functionalities. The Maillard reaction is a safe chemical method used to structurally modify proteins. The glycation can subsequently reduce the water loss of gels by improving the integrity of structure (Xia et al., 2023). It was also shown that the Maillard conjugates formed rubbery gels while non-conjugated polymers formed brittle gels (Meydani et al., 2019). The Maillard conjugates create a thick, continuous, and viscoelastic interfacial layer, stabilizing the system through both steric hindrance and electrostatic repulsions (Li et al., 2016; Yang et al., 2021). It was reported that the foaming properties of SPI increased after conjugation with gum arabic, sodium alginate, xanthan gum, and soybean polysaccharides (Zhang et al., 2024). In this regard, Maillard conjugates endow flavor-rich foods with high antioxidant, anti-inflammatory, and antiviral characteristics (Peng et al., 2021). The structural unfolding of proteins through Maillard reaction accelerate their migration to both water-oil and water-air interfaces since their absorption and rearrangement facilitates (Ke and Li, 2023). It was reported that Maillard reaction can improve the stability of both foams and emulsions (Choi et al., 2023).

Gellan gum, an anionic polysaccharide, has lower reducing power and greater steric hindrance compared to mono and disaccharides, leading to better control of Maillard reaction (Dev et al., 2021). However, low acyl gellan gum demands cations to form a robust gel. It was reported that high molecular weight conjugates with great viscosity can efficiently act as surfactants to entrap gas bubbles and reduce the drainage (Himashree et al., 2022). Moreover, since gelation through salt bridges occurs after denaturation/aggregation of biopolymers in cold-set gels, they possess greater structural homogeneity and water holding capacity (WHC) than heat-set gels (Meydani et al., 2019).

To date, aerated gels prepared by Maillard conjugates have not been studied. Therefore, the Maillard conjugates of SPI and gellan gum were used to boost the formation and stabilization of cold-induced aerated gels. Since aerated gels can satisfy consumers mouth feeling, and reduce the product cost and calorie (Zúñiga and Aguilera, 2008), the optimized aerated gel formed by SPI-gellan gum conjugate was used as an oil substitute in mayonnaise sauce to reduce the calorie. The literature review confirmed that the Maillard conjugates were not yet used to produce cold-set aerated gels, moreover, the aerated gel based on plant-derived protein was not yet substituted in mayonnaise sauce.

2. Materials and methods

2.1. Materials

SPI (>90% protein content, dry-based) and low acyl gellan gum (≥85% gellan content; 200–300 KDa) were purchased from Qindao Crown and Amstel products Co. (Netherland), respectively. Other chemicals were of analytical grade, bought from either Merck (Darmstadt, Germany) or Sigma Aldrich Co. (St Louis, MO, USA). Other ingredients of mayonnaise sauce were purchased from local groceries in Mashhad, Iran. All solutions were prepared with deionized water.

2.2. Description of study

The protein-gum conjugates of Maillard reaction were used to produce aerated gels with independent variables of SPI concentration (1.5, 2 and 2.5%), heating time (0, 45, and 90 min), and $CaCl_2$ concentration (100, 200, and 300 mM). The independent variables were selected as protein concentration greatly affects the characteristics of Maillard conjugates (Nooshkam et al., 2020) and composite gels (Kazemi-Taskooh and Varidi, 2024), heating time since Maillard duration significantly changes the glycation degree besides the functionalities of proteins (Chen et al., 2019), and $CaCl_2$ as the cation concentration greatly affects gelling properties (Gökmen and Şenyuva, 2007; Xiao et al., 2021).

The gels were optimized based on the features required for an acceptable mayonnaise sauce as the maximum hardness, WHC, and L^* but minimum density. The optimization was done by a numerical optimization using a central composite design, detailed in section 2.6. So, the optimized conditions were as follows: protein concentration of 1.5%, $CaCl_2$ of 300 mM, and heating time of 90 min. The conjugate formed at optimum point was assessed through Maillard products formation, pH, glycation degree, and SDS-PAGE. The optimized aerated gel was then characterized via FTIR, SEM, overrun, and rheology. Subsequently, the optimized aerated gel was incorporated in mayonnaise sauce with 0, 25, 50, 75, and 100% substitution as an oil substitute.

2.3. Maillard conjugates

Firstly, SPI was dissolved in sodium phosphate buffer (pH 7.5, 80 °C, 30 min) using a magnetic stirrer, cooled immediately in an ice-water bath and stored overnight (4 °C). The next day, gellan gum was dissolved in same buffer (60 °C, 30 min), then the gum solution was added to the SPI solution. The final concentrations of SPI were 1.5, 2 and 2.5% w/v, and that of gum was 1% w/v. Subsequently, the prepared solutions were subjected to a wet-heating treatment with continuous stirring at 90 °C for 0, 45, and 90 min. Finally, the samples were immediately cooled to 4 °C in an ice-water bath.

2.3.1. The intermediate and final products of Maillard reaction

The absorbance was recorded at 294 and 420 nm using a UV–Vis spectrophotometer (160 A Shimadzu, Kyoto, Japan) to investigate the intermediate and final products of Maillard reaction, respectively. The non-conjugated sample was used as blank (Nooshkam and Madadlou, 2016a).

2.3.2. pH

The pH value was measured before and after heating treatment (pHLab 827, Metrohm, Switzerland) at room temperature.

2.3.3. Glycation degree

The ortho-phthaldialdehyde reagent was used to record sample absorption at 340 nm (against water instead of sample) using an UV–Vis spectrophotometer (160 A Shimadzu, Kyoto, Japan). Then, the free amine groups were calculated based on L-Lysine calibration curve (0.02–0.16 mg/ml, $y = 3.2884x+0.058$, $R^2 = 0.99$) (Chailangka et al., 2022).

$$\text{Glycation degree} = \left(1 - \frac{\textit{free amine groups in conjugated sample}}{\textit{free amine groups in non} - \textit{conjugated sample}}\right) \times 100 \quad (1)$$

2.3.4. Sodium dodecyl sulfate-polyacrylamide gel electrophoresis (SDS-PAGE)

The discontinuous buffer system was used at 15% resolving gel and 5% stacking gel. An electrophoresis system (Bio-Rad Laboratories, Mini-Protean Tetra Cell Systems, Hercules, CA, USA) was utilized for 60 min at constant voltage of 160 V (Lavaei et al., 2022).

2.4. Aerated gels

For aeration, the conjugate solution (100 ml) was poured in a 250 ml plastic beaker. Calcium chloride ($CaCl_2$) (100, 200, and 300 mM) was then added, and immediately whipped (5000 rpm, 2 min) using a hand

mixer (Bosch, BS-378, 220 V, Germany) equipped with a wire whisk. The aerated structure was immediately cooled to 4 °C in an ice-water bath, and stored overnight (4 °C) to form aerated gels, and then characterized.

2.4.1. Density

A container (25 ml) was filled with gel, and cooled for 15 min.

$$Density\ (\rho) = \frac{Mass\ (g)}{Volume\ (ml)} \tag{2}$$

2.4.2. Color

The color parameters (L^*, a^*, and b^*) were measured using a digital colorimeter (Chroma meter CR-410, Konica Minolta, Japan).

2.4.3. Texture

The penetration test was applied with a penetration depth of 50% height using a 25 mm probe. The pre-test, test and post-test speeds were 1, 1, and 5 mm/s, respectively (TA.XT plus, Stable Microsystems, UK) (Tomczyńska-Mleko et al., 2022).

2.4.4. WHC

The gels were centrifuged (20 min, × 5000 *g*), the WHC was measured accordingly (Kazemi-Taskooh and Varidi, 2021).

$$WHC = \frac{Total\ water\ content\ before\ centrifugation\ (g) - released\ water\ (g)}{Total\ water\ content\ before\ centrifugation\ (g)} \tag{3}$$

2.4.5. Fourier transform-infrared (FTIR) spectroscopy

The spectra were recorded using a FTIR spectrophotometer (AVATAR-370, Thermo Nicolet, USA) at 400-4000 cm^{-1} (Zhao et al., 2021).

2.4.6. Microstructure

The freeze-dried gel was cut (5 × 5 mm) and coated with gold. The microstructure was imaged by a LEO, 1450 V P scanning electron microscope (Germany) (Ghasemi et al.) operated at 20 kV. The ImageJ software was used to analyze the pores (Kazemi-Taskooh and Varidi, 2021).

2.4.7. Overrun

A plastic container (25 ml) was filled with fresh gel sample, the sample surface was gently smoothed by a spatula. Then, the container was cooled down to form the gel and the overrun was calculated accordingly (Dehghannya et al., 2018):

$$Overrun\ (\%) = \frac{\left(\frac{1}{liquid\ density\ of\ aerated\ gel} - \frac{1}{aerated\ gel\ density}\right)}{\frac{1}{aerated\ gel\ density}} \tag{4}$$

2.4.8. Dynamic rheological measurements

A rheometer (MCR300, Anton Paar, Austria) was used to study strain sweep at 1 Hz and 25 °C to determine the viscoelastic linear region, which was found to be 0.5%. Then, the frequency sweep (0.01–10 Hz, 0.5% strain) and the temperature sweep (0–90 °C, 1 Hz, 0.5% strain) were tested to study storage modulus (G') and loss modulus (G"), which were fitted to Power-law equations.

$$G' = k' \times \omega^{n'} \tag{5}$$

$$G'' = k'' \times \omega^{n''} \tag{6}$$

$$Tan\ \delta = \frac{G''}{G'} \tag{7}$$

The k', n', k" and n" are the consistency index and flow behavior index of G' and G", respectively. The complex viscosity (η*) was also evaluated (Sun et al., 2018; Yu et al., 2020).

2.5. Mayonnaise sauce

To prepare 100 g sauce, dry ingredients (salt (0.6 g), white pepper (0.6 g), mustard (0.6 g), sugar (3 g)) were mixed with egg (8 g), water (10 g), lemon juice (3.56 g), and half of vinegar (6 g) for 3 min. Then, half of the oil was slowly added along with starch (1 g), xanthan gum (0.3 g), guar gum (0.3 g), and potassium sorbate (0.035). Subsequently, the other half of the oil was added, whipped (5000 rpm, 8 min) using a hand mixer (Bosch, BS-378, 220 V, Germany) equipped with a wire whisk. The other half of vinegar (6 g) was then added and whipped, and samples were kept in 4 °C for 2 min.

To reach the low-fat mayonnaise sauce, the oil was substituted (0, 25, 50, 75, and 100%) with the aerated gel produced in optimum conditions. Therefore, we had 5 samples in this section which contained 60, 45, 30, 15, and 0 g oil, respectively.

2.5.1. Proximate composition

The sauce composition was analyzed accordingly (Ghasemi et al., 2022). Finally, the sauce calorie was determined using equation (8) (Li et al., 2014):

$$Caloric\ Value\ \left[\frac{KCal}{100\ g}\right] = (Protein \times 4) + (Fat \times 9) + (Carb \times 4) \tag{8}$$

2.5.2. pH, color, texture

The parameters were experimented according to sections 2.3.2, 2.4.2, and 2.4.3, respectively.

2.5.3. Thermal stability

The sauce (3 g) was heated in a water bath (80 °C, 30 min), then centrifuged (7000 rpm, 10 min). The supernatant was removed and the remained sauce was weighed (Wang et al., 2022).

$$Thermal\ stability\ (\%) = \frac{Sauce\ weight\ after\ centrifugation}{Sauce\ weight\ before\ centrifugation} \times 100 \tag{9}$$

2.5.4. Storage stability

The fresh sauces (25 ml) were stored (4 °C), the images were taken by the optical microscopy in days 1, 7, and 14 (Olympus CX-41, Tokyo, Japan) with × 2000 magnification, quantified by ImageJ.

2.5.5. Sensory analysis

The quantitative descriptive analysis was applied to investigate the sensory parameters (color, smell, texture, flavor, overall acceptance) by 15 trained panelists. The fresh sauce samples were tested after 1 day of storage at 4 °C (Sun et al., 2018).

2.6. Statistical analysis

To characterize the aerated gels, the central composite design was used to investigate the effect of independent variables (heating time (0, 45, 90 min), protein concentration (1.5, 2, 2.5%), and $CaCl_2$ content (100, 200, and 300 mM)) on gel properties. The polynomial equation was applied by Design Expert13 software to relate the response with the independent variables. The response variables included density, color and texture parameters, and WHC. Hence, 17 experimental trials were analyzed (Table S1). As can be seen in Table S2, texture and color parameters were best fitted with quadratic model, but density and WHC were greatly fitted with the linear model. The R^2 and the R^2 adj of the models were between 0.92-0.99 and 0.90–0.98, respectively. Moreover, the lack of fit for all response variables showed the validity ($P>0.05$) and accuracy of the model in predicting responses (Ghobadi et al., 2018).

A numerical optimization was done by solving the inverse matrix of the polynomial regression equation by Design Expert13 software. The

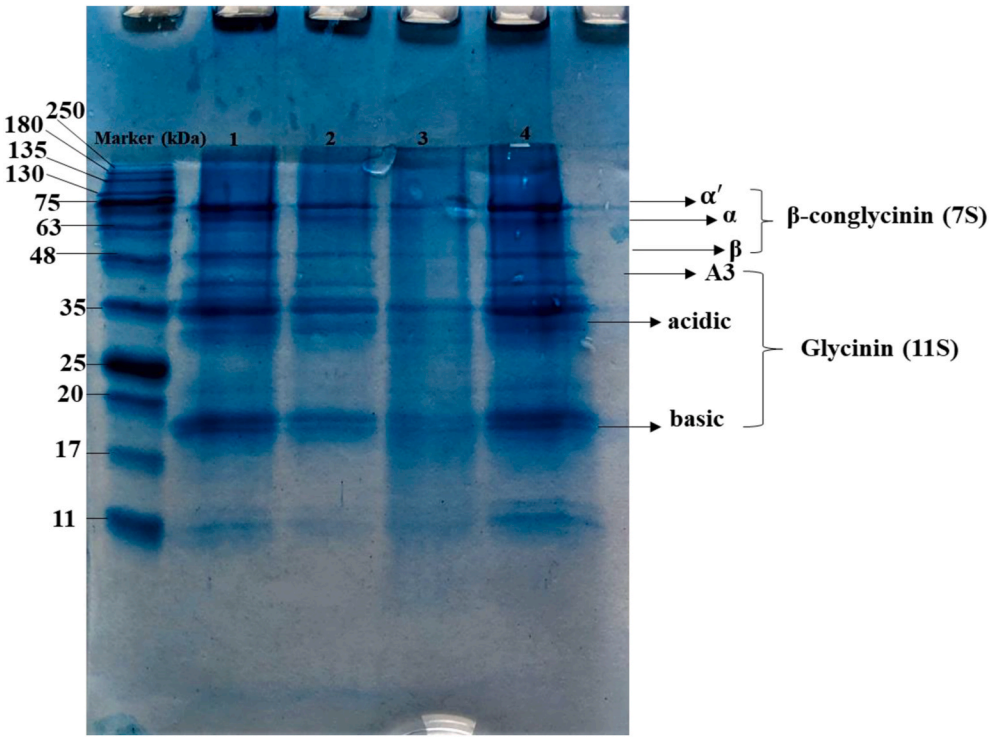

Fig. 1. The SDS-PAGE pattern of 1) unheated SPI, 2) SPI-gellan gum conjugate formed in optimum conditions, 3) non-conjugated SPI-gellan gum, and 4) heated SPI.

maximum hardness, WHC, and L^* but minimum density were statistically applied to determine the optimum point. To confirm the adequacy of the fit, the Student's t-test was applied, showing no significant difference between the actual and predicted values.

A completely randomized design was applied to investigate the effect of oil substitution (0, 25, 50, 75, and 100%) with optimized aerated gel in a factorial arrangement using SPSS26 software. Significant differences between the means were analyzed by Duncan test at $P<0.05$. All experiments were done in triplicate, and the results were recorded as mean ± standard deviation.

3. Results and discussion

3.1. Maillard conjugate

The conjugate was produced in optimum conditions as follows: SPI 1.5%, gellan gum 1%, and heating time of 90 min, then compared with the non-conjugated sample in same concentrations without heat-treatment. The absorptions at 294 and 420 nm were 0.306 ± 0.002 and 0.096 ± 0.001, showing the intermediate and final products of Maillard, respectively. The amine groups involved in the conjugation produced acidic compounds, causing a high absorption at 294 nm. Since the absorption at 294 nm was higher than absorption at 420 nm, the Maillard reaction was probably in the early stages. The similar results were previously reported in α-lactalbumin with glucose, maltotriose, maltopentaose and maltoheptaose, cricket protein and fructo-oligosaccharides (Chailangka et al., 2022), WPI- or SPI-gellan gum conjugates (Lavaei et al., 2022). On the other hand, low melanoidin production caused a low absorbance at 420 nm which points to the controlled condition of the Maillard reaction in our system.

The pH of non-conjugated sample was 7.45 ± 0.007 which decreased to 6.94 ± 0.007 in conjugated sample, confirming the conjugation between SPI and gellan gum. Consumption of free amino groups produced acetic acid, formic acid, methylglyoxal, and glyoxal, so the pH decreased during the Maillard reaction. Likewise, the pH of WPI- and SPI-gellan gum Maillard-driven conjugates changed from 7 to 6.82 and 6.84, respectively (Lavaei et al., 2022).

The progress of Maillard reaction was also assessed with glycation degree which was 36.5 ± 0.07% in SPI-gellan gum conjugate. Indeed, various factors affected the reduced glycation degree: I) increased denaturation of protein and releasing more amino groups, II) decreased availability of reducing agents, and III) saturation of active sites (Ajandouz et al., 2001). By increasing heating time, protein unfolded, more ε-amino groups were available to be covalently bonded with polysaccharide (Chailangka et al., 2022). Subsequently, the amino groups of proteins along with carbonyl groups of polysaccharides were consumed during extended heating time.

The SDS-PAGE method was performed (Fig. 1) to study the electrophoretic pattern of conjugated sample. The subunits of SPI consist of glycinin and β-conglycinin. The glycinin as a heterogeneous oligomeric protein contains 6 acidic polypeptide chains (35–45 KDa) and 6 basic polypeptides (18–20 KDa), while β-conglycinin as a heterogeneous glycoprotein contains subunits called α', α, and β with molecular weight of 72, 68, and 52 KDa, respectively (Y. Yang et al., 2020). As can be seen in lane 4, SPI denatured upon heating, so the bands at 180 and 250 KDa were intensified. Furthermore, comparison of lane 1 (unheated SPI) to lane 4 (heated SPI) showed that the 75, 180, and 250 KDa bands became darker. The phenomenon was attributed to the protein aggregations upon disulfide and noncovalent bonds (Pi et al., 2023). Since conjugation occurred (lane 2), the intensity of lower molecular weight protein fractions were significantly reduced (lanes 1, 3, and 4), confirming structural changes of SPI during Maillard reaction. Similarly, characteristic bands of SPI were disappeared upon conjugation with maltose on a wet heat treatment (48–72 h). Moreover, high molecular weight conjugates produced through Maillard reaction were remained at the top of injection wells, and could not diffuse into the resolving gel (Chailangka et al., 2022).

3.2. Aerated gels

3.2.1. Density

The effect of reciprocal effects of independent variables on gel

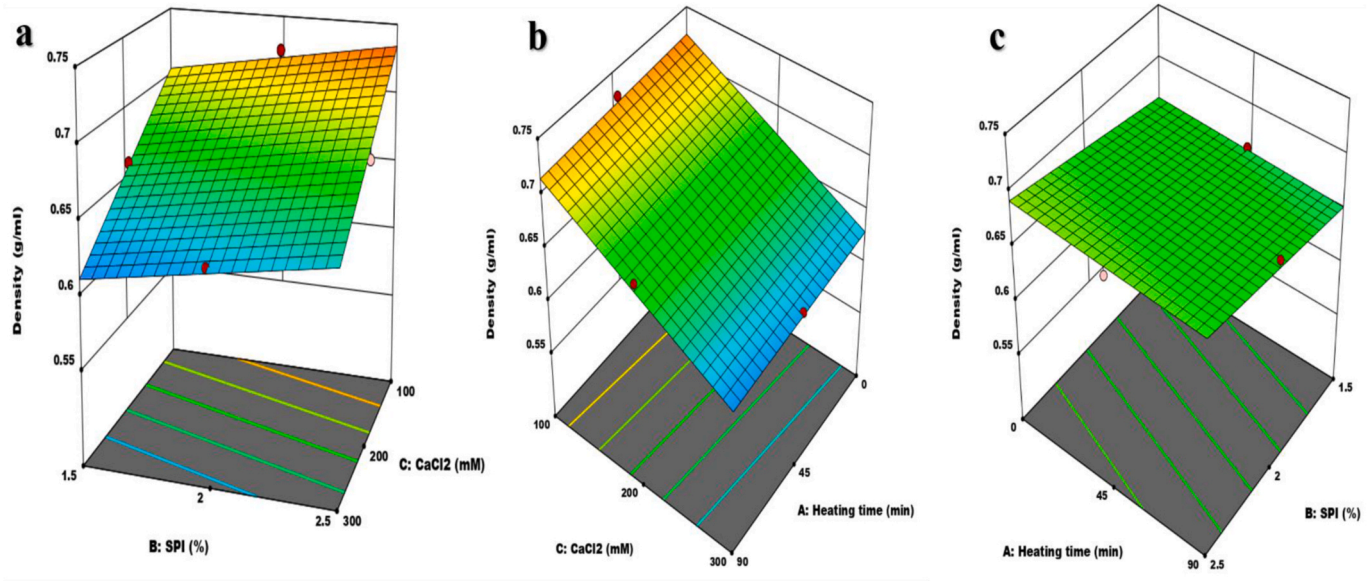

Fig. 2. Response surface of the effect of a) SPI - $CaCl_2$, b) heating time- $CaCl_2$, c) heating time –SPI on binary gel density.

density were presented in Fig. 2. The gel density increased upon increasing SPI concentration ($P<0.01$), pointing to the fact that SPI migration to the air-water interface was slowed down. It was stated that excessive polymer concentrations along with high amount of hydrophobic interactions can weaken the network (Kazemi-Taskooh and Varidi, 2024). So, protein-protein interactivities probably caused some aggregations which reduced foamability regarding the decreased surface activity (Li et al., 2022). In this context, sodium caseinates could not form foam-based structures since biopolymer adsorption in the interface greatly depends on its concentration (Sánchez and Patino, 2005).

Entrapment of high volume of air bubbles decreases the density, which was observed upon increasing $CaCl_2$ concentration from 100 to 300 mM ($P<0.01$). The density decreased (18%) by increasing $CaCl_2$ content. The excessive ionic amino acids at protein surface were electrostatically shielded by $CaCl_2$, the biopolymers tendency toward water decreased which accelerated their absorption at the interface. Subsequently, the surface activity of biopolymers increased since the free energy of Gibbs was reduced upon biopolymer migration to the interface, and the biopolymers stability increased at the air-water interface (Damodaran, 2017; Zheng et al., 2023). Therefore, the surface tension declined, resulting in reduced density. Further, increasing heating time (0–90 min) decreased the density ($P<0.05$) since conjugation could increase the foaming capacity. Indeed, the surface tension at air-water interface decreased by modifying the surface hydrophobicity of proteins using Maillard reaction (Nooshkam and Madadlou, 2016b).

3.2.2. Color

Reduction of air bubbles decreased brightness and light scattering and b^* (41.42%) ($P < 0.05$) but enhanced a^* ($P<0.01$) and density upon increasing SPI concentration. Hence, there was a negative correlation between L^* and density. Researchers reported that integration of air bubbles affects the refraction and light scattering (Jakubczyk and Kamińska-Dwórznicka, 2021). Likewise, the L^* decreased by increasing SPI concentration in cold-set protein gels (Maltais et al., 2005). The effect of reciprocal effects of independent variables on color parameters were presented in Fig. 3. Moreover, the effect of $CaCl_2$ concentration on all color parameters was statistically significant ($P<0.01$), the a^* increased (37%) but the b^* decreased. Increasing $CaCl_2$ concentration improved L^* (14.5%) which was in agreement with density reduction as more air bubbles were entrapped in the gel. Similarly, L^* increased but b^* decreased by increasing $CaCl_2$ content in glycinin and conglycinin gels, pointing to more aggregated and denser structures (Maltais et al., 2005).

Increasing heating time and further progress of Maillard reaction improved L^* ($P<0.05$) and b^* but reduced a^* ($P<0.01$). All of which were related to decomposition of brown products during intermediate levels of Maillard reaction along with production of yellowish and colored compounds with nitrogen in advanced levels. Similarly, decomposition of light-absorbing products such as chromophores improved the L^* in SPI-gellan gum emulsion gels (Lavaei et al., 2022). It was proved that increasing light scattering and refraction in aerated structures occur upon increasing air bubbles (Jakubczyk and Kamińska-Dwórznicka, 2021), resulting in density reduction which was similar to our results.

3.2.3. Texture

Increasing protein concentration reduced hardness and adhesiveness ($P<0.05$) but increased the cohesiveness ($P<0.05$) of aerated gels. The effect of reciprocal effects of independent variables on textural characteristics were presented in Fig. 4. It was reported that adhesiveness reduction by increasing whey protein concentration in cold-set gels occurred due to the formation of a non-integrated gel structure (Lee and Jo, 2023). Subsequently, protein molecules aggregated and did not participate in gel matrix (Totosaus et al., 2002), decreasing the hardness and cohesiveness. It can, hence, be concluded that improvement of mechanical features of a binary gel demands a critical mass ratio of protein/polysaccharide, so higher amounts of biopolymers reduces the gel properties (Kazemi-Taskooh and Varidi, 2024). It was also reported that excessive hydrophobic forces and sulfhydryl-disulfide interchanges increased aggregations among proteins, besides, increased molecular weight of polymers reduced the reaction kinetics (Spotti et al., 2019), which probably occurred in our system to reduce the hardness. Increasing $CaCl_2$ concentration from 100 to 200 mM improved the textural characteristics ($P<0.05$) regarding the formation of electrostatic interactions among biopolymers. However, further introduction of calcium ions (200–300 mM) weakened the gel structure ($P<0.05$). The phenomenon was previously reported in cold-induced whey protein isolate (WPI) gels. Therefore, the textural properties of aerated gel decreased. It was proved that increased cross-linking degree improved the gel strength (Spotti et al., 2019), so it can be speculated that excessive $CaCl_2$ contents could not cross link the macromolecules. All of which probably reduced the gel homogeneity, decreasing the textural parameters.

However, increasing heating time improved hardness and

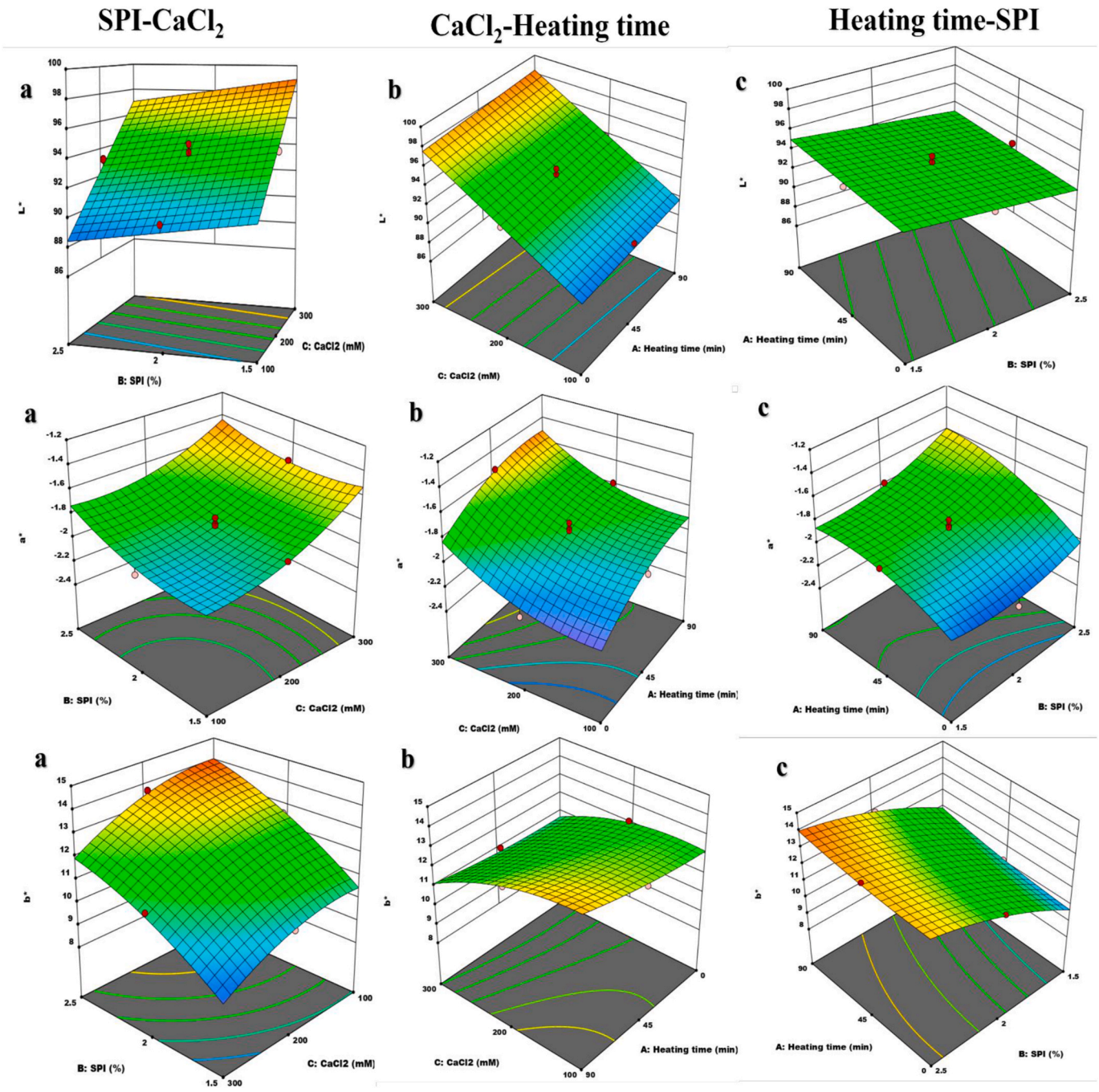

Fig. 3. Response surface of the effect of independent variables on color parameters: a) L^*, b) a^*, and c) b^* of aerated gels.

adhesiveness but decreased cohesiveness ($P < 0.05$). The amino groups were consumed through Maillard reaction which decreased the electrostatic repulsions, improving the hardness (Wen-qiong et al., 2021) and adhesiveness. Indeed, polysaccharides chemically modify the secondary and teriary structures of proteins as accelerate the transition of α-helices to β-sheets, which enhances both hydrogen bonds and hydrophobic forces. It was also shown that gelation is directly related with the β-sheet content (Kazemi-Taskooh and Varidi, 2024). Similarly, the β-sheets of pea protein increased after conjugation with xanthan gum (Choi et al., 2023). Thus, it could be concluded that SPI structure was probably better unfolded by simultaneous impact of gellan gum and heating time, which facilitated gelation through hydrogen and hydrophobic interactivities. So, a more compact uniform network formed by increasing heating time, resulted in enhanced hardness.

3.2.4. WHC

The WHC is a functional property indicating the physical holding of water in a network which is significantly influenced by concentration and type of macromolecules, pore size, and experimental factors (time and applied forces) (Kazemi-Taskooh and Varidi, 2023). Increasing SPI concentration improved the WHC ($P<0.05$) since higher protein content provided more hydrophilic groups interacting with water molecules (Kuhn et al., 2010). The effect of reciprocal effects of independent variables on WHC were presented in Fig. 5. It was reported that more fine-stranded gels with less dense aggregates improve the WHC (Ma et al., 2019). Likewise, the polar amino acids of SPI were the main water binding sites in SPI cold-set gels, improving the WHC (Maltais et al., 2005; Villanueva et al., 2018). The WHC increased (25%) by increasing $CaCl_2$ concentration ($P<0.01$) similar to previous research on cold-set

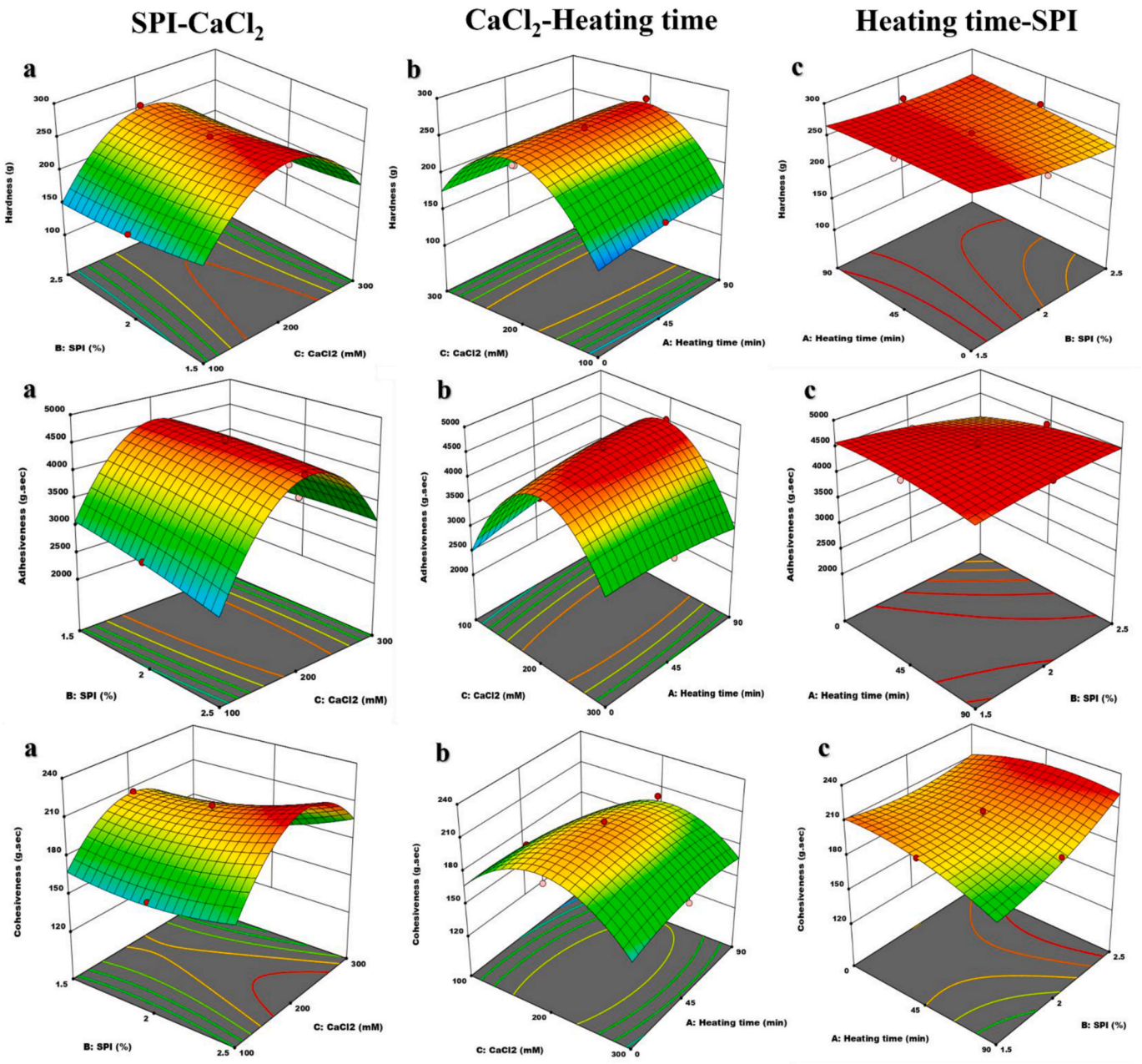

Fig. 4. Response surface of the effect of independent variables on texture parameters: a) hardness, b) cohesiveness, c) adhesiveness of aerated gels.

SPI hydrogels (Maltais et al., 2005). Divalent ions form salt bridges between biopolymers, structuralizing the gel network and stabilizing the water molecules. Thus, the WHC improves (Kuhn et al., 2010). It is proved that higher WHC causes more light scattering (Petcharat and Benjakul, 2017), which was observed in our aerated gels. By increasing $CaCl_2$ concentration, WHC, hardness, and L^* were simultaneously improved.

On the other hand, increasing heating time decreased the WHC ($P<0.05$). It was previously hypothesized that the protein structure changed during conjugation, the surface hydrophobicity subsequently increased, the SPI-maltodextrin interactions decreased, larger pores were formed, and the gel lattice was weakened, so the molecular interactions in the gel structure and eventually the WHC decreased (Zhao et al., 2021). The surface hydrophobicity reduction through dry-heating was well-correlated with WHC improvement in SPI-maltodextrin networks. While, the WHC decreased in wet-heating (Boonlao et al., 2023) similar to ours. Furthermore, sulfhydryl groups might be blocked by Maillard products which similarly decreased the WHC in myofibrillar gels (Peng et al., 2021).

3.2.5. FTIR

As can be seen in Fig. 6, the wavenumber of amides I, II, and III of SPI spectrum were 1643 cm^{-1} (1600-1700 cm^{-1}, C=O stretching vibrations), 1515 cm^{-1} (1450-1550 cm^{-1}, N-H bending and C-H stretching vibrations), and 1236-1442 cm^{-1} (1200-1450 cm^{-1}, C-N stretching and N-H bending vibrations), respectively. Moreover, the prominent absorption bands of gellan gum were seen at 605 cm^{-1} known as the skeletal region (long biopolymer chains), 1020 cm^{-1} (bending vibrations of the end of the chain), 1407 cm^{-1} (C-O stretching vibrations), 1592 cm^{-1} (C=O stretching vibrations), and 3370 cm^{-1} (O-H stretching vibrations). Further, the main bands of $CaCl_2.2H_2O$ were seen at 2129 and 1625 cm^{-1} (H-O-H composite bending bond), and 3423 cm^{-1} (O-H asymmetric stretching) (Karunadasa et al., 2018; Lavaei et al., 2022). Amide I and II bands shifted from 1648 to 1623 cm^{-1}, and 1515 to 1590

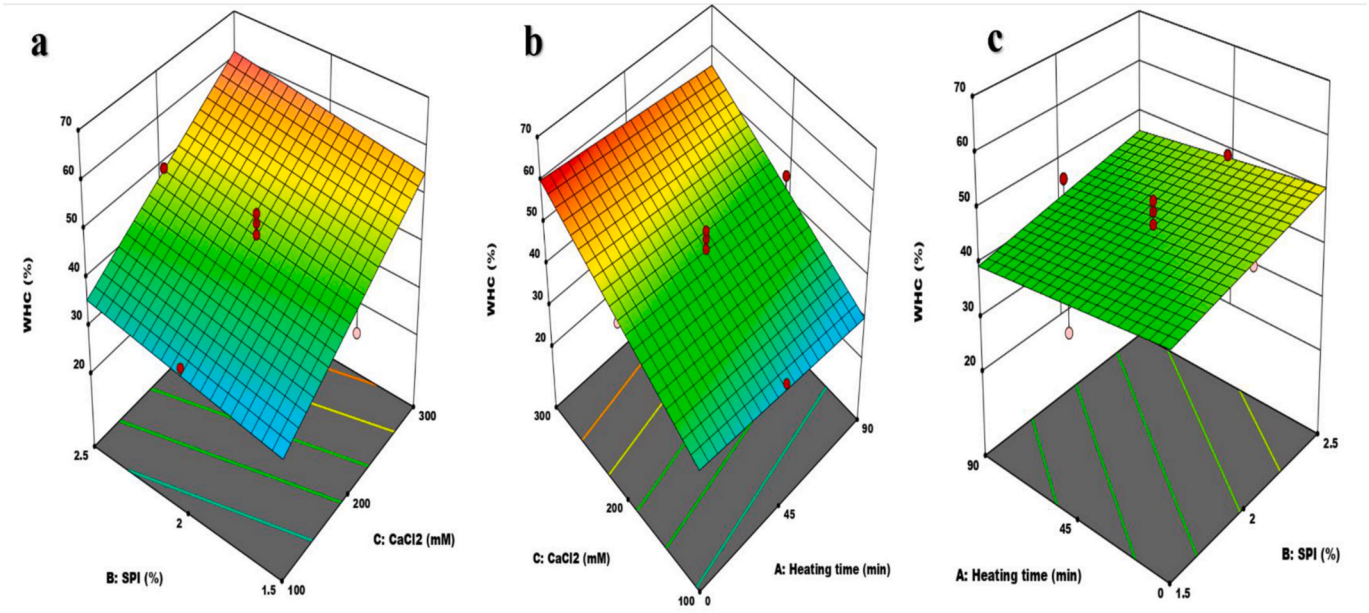

Fig. 5. Response surface of the effect of independent variables on WHC: a) SPI-$CaCl_2$, b) heating time-$CaCl_2$, c) heating time-SPI.

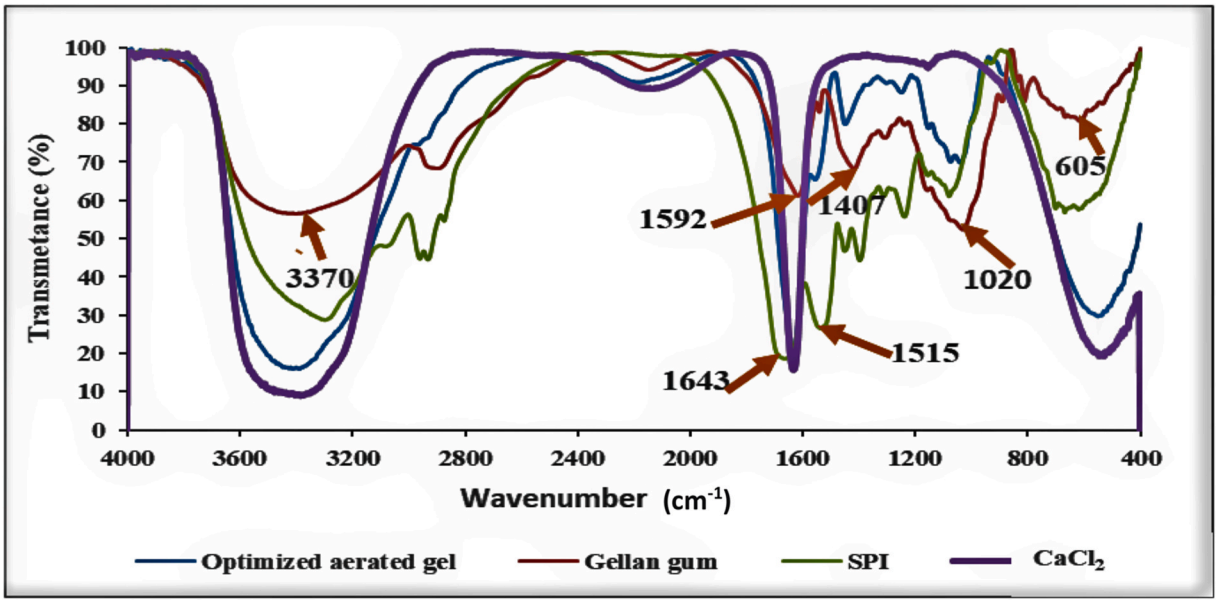

Fig. 6. The FTIR spectra of SPI, gellan gum, $CaCl_2$, and optimized aerated gel.

cm^{-1}, resulted from various mechanisms: I) consumption and formation of some functional groups during Maillard reaction, II) changes of the space around the amine groups of the protein due to the interactions with carboxyl groups of gellan gum, and III) $CaCl_2$ addition that might affect the secondary structures of aggregates. Also, the intensity of amide III band decreased because of glycation. Besides, $CaCl_2$ possibly prevented formation of additional intermolecular N–H•••O=C hydrogen bonds since Cl^- can act as a good proton receptor of NH (Miao et al., 2023). Similarly, a broad band was reported in cold-set soy protein gel between 1675 and 1625 cm^{-1}. The deconvolution subsequently showed enhancement of β-sheet contents after glycation (Maltais et al., 2008).

It is also proved that Maillard reaction can decrease the frequency of stretching vibrations of C=O (1648 cm^{-1}) and increase the bending vibrations of N-H, showing the formation of hydrogen bonds. The new peaks in the wavenumber range of 500–530 cm^{-1} indicate the oxidation of sulfhydryl groups (S-S stretching vibrations) in Maillard reaction, and the intensity of these peaks can be attributed to partial denaturation of protein, increasing protein-protein interactions, and reducing the number of NH_2 groups during the heating time. The wavenumber of 750–900 cm^{-1} (fingerprint area of polysaccharides) in gellan gum spectrum corresponded to the anomeric region of saccharide configuration, the intensity of which decreased in aerated gel, showing that the gum and protein were bonded. Furthermore, the peak at 1020 cm^{-1} in gellan gum spectrum was attributed to the glycosidic linkage, the intensity of which decreased after glycation (Nooshkam and Madadlou, 2016a; Sheng et al., 2020). The increase in the intensity of the aerated gel bands in the range of 3203–3606 cm^{-1} demonstrated O-H stretching vibrations and confirmed the covalent binding of SPI and gellan gum with high hydroxyl groups (Sheng et al., 2020). Furthermore, the 2900 cm^{-1} area in the spectrum of aerated gel indicates C-H stretching vibrations, pointing to the increase of protein surface hydrophobicity

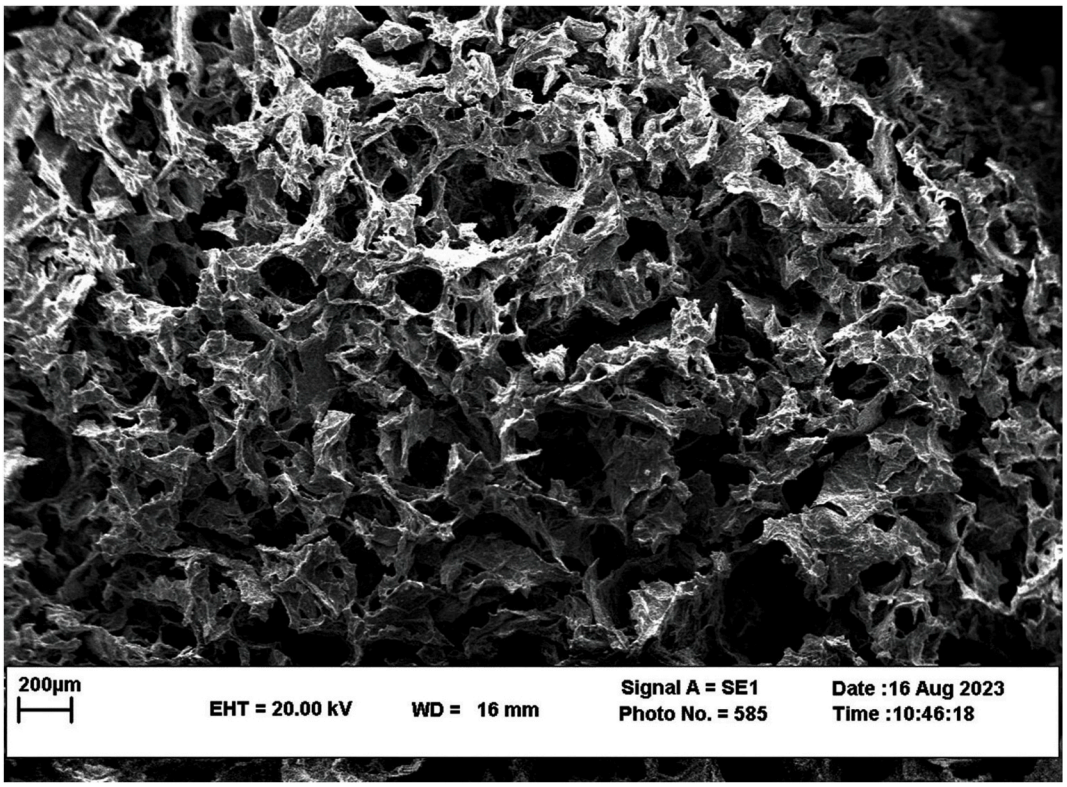

Fig. 7. The SEM image of optimized aerated gel.

(Miao et al., 2023). Interestingly, a new peak appeared at 1648 cm^{-1} in the aerated gel spectrum, showing stretching vibrations of C=N band of Schiff base formed between protein-gum (Chailangka et al., 2022), which was consistent with the results of absorptions at 294 and 420 nm.

3.2.6. SEM

Small, flat, and compact air pores were imaged via SEM (Fig. 7). The microstructure was consistent with great WHC (52%), high hardness (175.62 g) and L^* (99) since small pores provided great hardness but a large number of the pores resulted light refraction and scattering. The ImageJ determined the average and the maximum diameter of the pores as 61.52 ± 1.36 and 15 µm, respectively. Similar to SPI-gellan gum samples (Vilela et al., 2011), a thick protein-polysaccharide wall along with $CaCl_2$ connections were observed. In this context, it was explained that superior gel integrity resulting in homogeneous microstructure originates from enhanced H-bonds which improves the mechanical attributes (Kazemi-Taskooh and Varidi, 2023), which was in line with FTIR results.

3.2.7. Overrun

The conjugated gel exhibited 20.8% higher overrun but 3% lower density compared with the non-conjugated gel, showing increased air bubbles within the structure. Indeed, the reduction of surface and interfacial tension by increasing the hydrophobic interactions at air-water interface improved the aeration and foamability through Maillard conjugation. Briefly, gellan gum probably modified the surface hydrophobicity of SPI, so more hydrophobic amino acids were exposed to SPI surface. Thus, the hydrophilic/hydrophobic balance was adjusted through glycation (Ma et al., 2022). Improvement of protein solubility through Maillard reaction facilitates the surface adsorption during whipping. In this context, foaming capacity and stability of SPI-maltodextrin were improved as heat treatment increased from 30 to 60 min. It was shown that enhancement of secondary random structures in SPI improved the solubility (Boonlao et al., 2023).

3.2.8. Rheology

3.2.8.1. Strain sweep. The strain sweep test determined the average elastic and viscous modulus (G′ and G″) as 745.6 ± 0.01 and 176.92 ± 0.89 Pa, respectively. As can be seen in Fig. 8-a, the viscoelastic modulus-strain plot represented two separable areas where: I) G′ was parallel but higher than G″ with constant values, indicating linear viscoelastic region, pointing to the solid-like behavior of our optimized aerated gel, and II) a non-linear intersecting area with an inverse relation between strain with G' or G". After the intersection of modulus, the viscous modulus increased followed by a reduction. Therefore, the behavior of the sample was weak strain overshoot which indicates the high structural complexity of the sample (Hyun et al., 2002). The strong and weak gels are distinguishable based on strain sweep test. A weak gel does not remain in linear viscoelastic region by increasing strain (Kazemi-Taskooh and Varidi, 2023) which was observed in our gel.

Similar to our results, the G′ and G″ of SPI-κ-carrageenan acid-induced gels were in the steady state in strain <1%, indicating the linear viscoelastic region. Increasing strain over the critical point of 1–2% declined both G′ and G". Afterward, the critical point value of strain decreased at the high speed shear rate (14000 N) regarding the reduction of gel strength (Bi et al., 2018). Besides, increasing G' and G" of SPI gels were attributed to the morphological and flexibility changes of protein structure during heat treatment (Huang et al., 2022). As the average loss tangent (tan δ) was 0.23 ± 0.0014 (between 0.1 and 1), our aerated gel structure was between a real gel (tan δ < 0.1) and a high-concentrated weak elastic gel (Mandala et al., 2004). Hence, the sample was a typical gel network.

3.2.8.2. Frequency sweep. The G′ and G″ were slightly dependent on frequency in the linear viscoelastic region by a completely parallel pattern. Subsequently, the G′ and G″ were fitted to Power-law model (R^2 = 0.93–0.99), the n' and n" were 0.08 ± 0.14 and 0.15 ± 0.014 along with the k' and k" of 867.45 ± 0.69 and 109.10 ± 1.27 Pa. s^n,

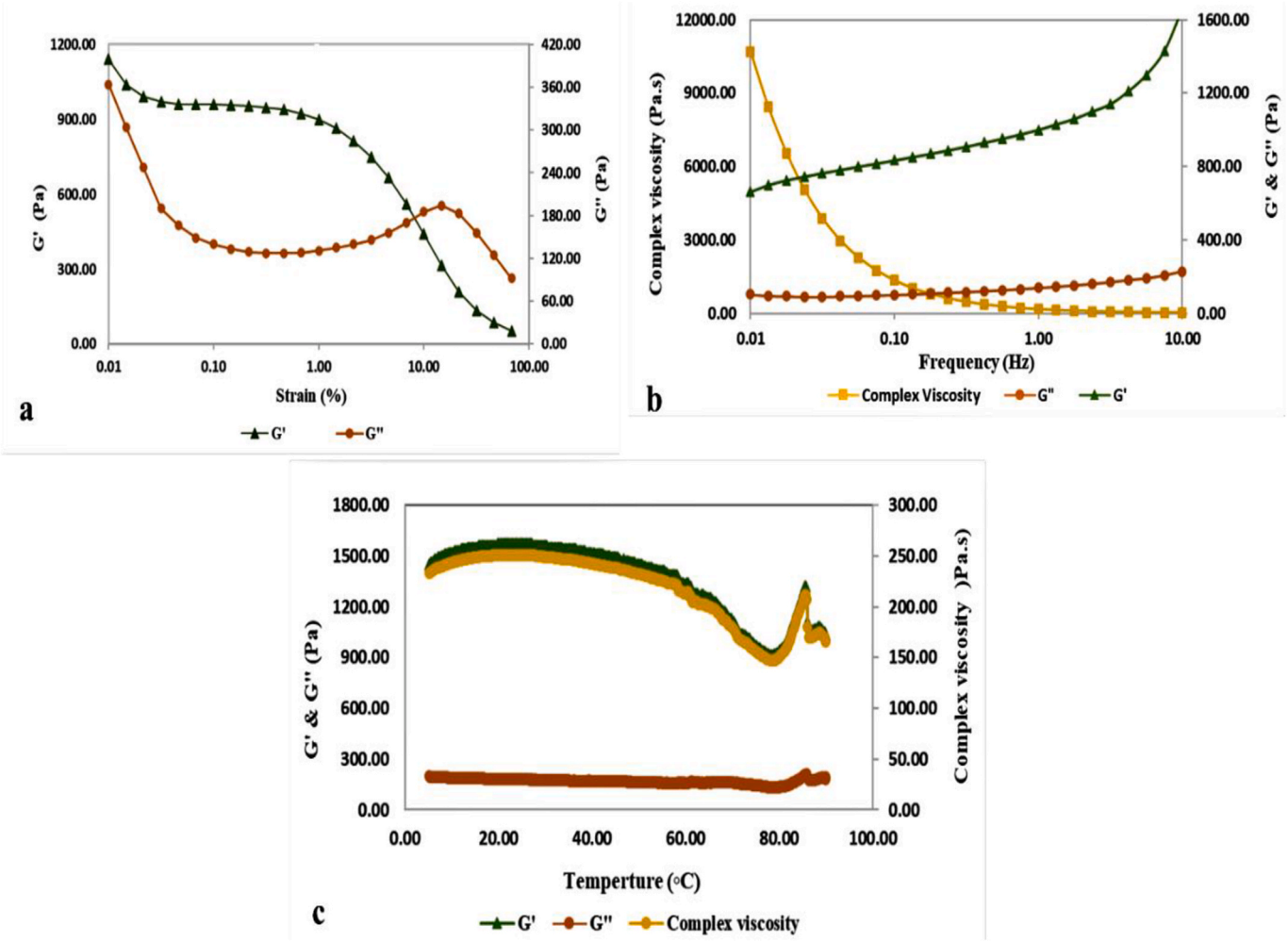

Fig. 8. Rheological properties of optimized aerated gel: a) strain sweep, b) frequency sweep, c) temperature sweep.

respectively. The tan δ < 1 and >1 identify more elastic and viscous behavior, respectively (Heydari and Razavi, 2021). Our gel showed more elasticity than viscosity as k'>k", confirmed by G'>G″ at all frequencies and tan δ of 0.13 ± 0.01. Moreover, the n values were between 0 and 1, presenting a pseudoplastic behavior. It might be concluded that covalent crosslinking was dominated in optimized aerated gel sample (Derkach et al., 2020). It was shown that heat treatment (95 °C, 20 min) enhanced both G′ and G″ of SPI gels compared with unheated samples (Huang et al., 2022), which could be due to the formation of new interactions like covalent crosslinks and hydrogen bonds. Likewise, the G" of SPI emulsion gels induced by $CaSO_4$ was lower than G′ by a parallel profile in frequency sweep test (1–100 Hz, strain 1%). Besides, the n was near zero (0.09), revealing slight dependency of modulus to angular frequency. Thus, the structure was formed by noncovalent/physical cross-linkages. However, the larger or more protein aggregation in the structure, the lower the n values and the higher the G'. So, a homogeneous stable emulsion gel was formed with strong viscoelastic properties (Wang et al., 2017).

The frequency sweep results of optimized gel were in accordance with hardness (177.92 g), cohesiveness (2612.66 g s), WHC (52%), and SEM images (uniform structure). Hence, it can be concluded that our optimized aerated gel sample was a weak elastic gel consisting of both covalent and noncovalent interactions. Indeed, Maillard reaction formed covalent bonds, $CaCl_2$ induced noncovalent crosslinks, and protein-gum had also physical entanglements. All of which caused gelation in our system. The frequency sweep results were in line with the strain ones. The complex viscosity (η*) decreased upon increasing the frequency on logarithmic-logarithmic scale with a slope of −0.89, similar to the value of concentrated commercial polysaccharides (−0.76). Based on η*, our gel was also formed upon entanglement of the chains (Alghooneh et al., 2018). Similarly, the η* of egg albumin-sesbania gum gels decreased as frequency increased (1–100 Hz) but both modulus increased (Li et al., 2020).

3.2.8.3. Temperature sweep. Increasing temperature from 5 to 40, 80, and 85 °C respectively increased, slightly decreased and then sharply increased all parameters (G′, G″ and η*) (Fig. 8-c). High temperature (80 °C) might slightly destroy the air bubbles which were significantly trapped in the structure (evidenced by density and overrun, sections 3.2.1 and 3.2.7, respectively). Likewise, the G′ and G″ of quinoa protein isolate-guar and locust bean gum gels slightly increased at 85 °C regarding the fact that protein denatured and unfolded, so hydrophobic amino groups buried inside the protein were exposed, and eventually proteins aggregated (Patole et al., 2022). It is worth mentioning that the aerated gel was thermally stable up to 90 °C. It could be due to the interactivities between SPI and gellan gum (like covalent crosslinks, confirmed by intermediate products of Maillard, glycation degree of 35%, and high molecular weight conjugates at SDS-PAGE) that could help the protein structure to remain stable against temperature. Similarly, conjugates of WPI-gum acacia (50–70 °C) formed thermally stable emulsions compared with single protein samples, due to the steric hindrance and electrostatic inhibition by anionic polysaccharide with long chains (Chen et al., 2019). Finally, all parameters (G', G", and η*) were reduced at temperatures higher than 90 °C as protein denatured.

Table 1
Proximate composition and caloric values of mayonnaise sauce.

Treatments	Moisture (%)	Protein (%)	Carbohydrate (%)	Ash (%)	Fat (%)	Caloric values (KCal/100 g)
S-0%	31.31 ± 0.30^{a}	1.80 ± 0.01^{a}	6.58 ± 1.19^{a}	0.92 ± 0.007^{a}	59.37 ± 0.88^{e}	567.91 ± 3.17^{e}
S-25%	41.41 ± 1.21^{b}	1.89 ± 0.01^{b}	7.35 ± 3.05^{ab}	1.17 ± 0.01^{b}	46.94 ± 2.53^{d}	462.52 ± 10.31^{d}
S-50%	51.5 ± 2.13^{c}	1.98 ± 0.02^{c}	10.56 ± 2.07^{abc}	1.42 ± 0.01^{c}	34.52 ± 4.19^{c}	348.06 ± 25.43^{c}
S-75%	66.59 ± 2.07^{d}	2.13 ± 0.02^{d}	11.89 ± 0.20^{bc}	1.87 ± 0.02^{d}	17.51 ± 2.05^{b}	215.15 ± 20.83^{b}
S-100%	82.58 ± 0.53^{e}	2.28 ± 0.02^{e}	12.24 ± 0.61^{c}	2.33 ± 0.04^{e}	0.51 ± 0.07^{c}	62.87 ± 1.83^{a}

Means within the same column with different superscripts differ significantly ($P<0.05$).

Table 2
Characterization of mayonnaise sauce.

Treatments	pH	L^*	a^*	b^*	Hardness (g)	Cohesiveness (g.s)	Adhesiveness (g.s)
S-0%	3.93 ± 0.02^{a}	95.23 ± 0.16^{e}	-6.16 ± 0.04^{a}	25.27 ± 0.03^{a}	81.48 ± 0.94^{c}	155.96 ± 1.70^{c}	1189.76 ± 4.44^{e}
S-25%	3.96 ± 0.01^{b}	93.54 ± 0.29^{d}	-6.24 ± 0.49^{a}	25.09 ± 0.98^{a}	72.57 ± 6.40^{bc}	112.52 ± 8.05^{b}	1146.06 ± 19.72^{d}
S-50%	3.99 ± 0.01^{c}	92.20 ± 0.24^{c}	-6.37 ± 0.18^{a}	28.80 ± 0.96^{b}	61.45 ± 7.69^{ab}	101.01 ± 8.47^{b}	1046.64 ± 4.74^{c}
S-75%	4.04 ± 0.01^{d}	89.25 ± 0.12^{b}	-5.93 ± 0.14^{b}	31.66 ± 0.18^{c}	53.98 ± 3.13^{a}	85.70 ± 1.10^{a}	833.52 ± 6.15^{b}
S-100%	4.05 ± 0.02^{d}	84.55 ± 0.16^{a}	-5.25 ± 0.01^{c}	35.28 ± 0.16^{d}	58.31 ± 1.33^{a}	82.63 ± 1.63^{a}	946.34 ± 2.58^{a}

Means within the same column with different superscripts differ significantly ($P<0.05$).

3.3. Mayonnaise sauce

3.3.1. Proximate composition

By increasing the aerated gel in sauce samples, moisture, protein, carbohydrate, and ash contents significantly increased whereas the caloric value decreased ($P<0.05$) (Table 1). The ash amount could be due to the presence of $CaCl_2$ and protein/gum impurities. Our results were in agreement with other studies on substitution of mayonnaise oil with zein or WPI-pectin gel (Sun et al., 2018).

3.3.2. pH

The pH of mayonnaise sauce is a critical factor that should not exceed from 4.1 since higher pHs cause pathogenic microbial growth like *Staphylococcus aureus*. Although the pH of our aerated gel was neutral, the final pH of sauce samples remained in the range (Table 2). The pH increased by increasing aerated gel substitution ($P<0.05$), related with enhancement of moisture content. Other studies on replacement of chitosan, tamarind and chitin in low fat mayonnaise showed similar results (Al-Aubadi, 2021).

3.3.3. Color

Increasing the amount of substitution reduced L^* ($P<0.05$, Table 2) as droplet size increased (section 3.4.6), resulting in decreased light scattering while light absorption/transmission increased by air bubbles. Likewise, increasing modified wheat starch in O/W emulsions instead of oil reduced the light scattering (Heydari and Razavi, 2021). The results of a^* demonstrated a decrease ($P<0.05$) in 75% and 100% substitution samples accompanied with higher moisture. Indeed, the fat-soluble pigments were diluted similar to oil substitution of mayonnaise sauce with pectin-WPI gels (Sun et al., 2018). Subsequently, the b^* increased by 28.38% as substitution increased, pointing to higher yellowness, probably resulted from Maillard products.

3.3.4. Texture

As oil content decreased, hardness (81.48 ± 0.94 to 58.31 ± 1.33 g), cohesiveness (1189.76 ± 4.44 to 946.34 ± 2.58 g s), and adhesiveness (155.96 ± 1.7 to 82.63 ± 1.63 g s) decreased compared to the control (S-0%) (Table 2). The reduced mechanical characteristics was attributed to the enhancement of air bubbles and aqueous phase (Herremans et al., 2013; Nikzade et al., 2012). It can be concluded that the harder the mayonnaise, the finer the oil distribution in the continuous phase. As a result, mayonnaise with more finely dispersed oil tends to be harder than mayonnaise with a lower fat content. As can be seen in Fig. 9, the oil droplets became larger by increasing substitution. Indeed, the textural parameters were negatively correlated with droplet size. Likewise, hardness and cohesiveness decreased upon substitution of chia mucilage (4%) as an oil replacer of O/W emulsions, so droplet size increased (Heydari and Razavi, 2021) which was in agreement with present work.

3.3.5. Thermal stability

The thermal stability increased ($P<0.05$, Table 3) by 29.11% compared to the control as substitution increased up to 75%. It was proved that electrostatic interactions and steric hindrance are the main stabilizing forces within an emulsion (Park et al., 2020). Hence, SPI-gellan gum conjugates probably created steric hindrance and ionic interactivities, forming a thick layer around the oil-water droplets and air bubbles to prevent flocculation or coalescence. Likewise, pectin, starch and xanthan addition in mayonnaise sauces improved the thermal stability of samples due to the fact that movements of oil droplets were restricted by increasing the viscosity (Wang et al., 2022). However, the thermal stability decreased upon 100% substitution as biopolymers probably could not be adsorbed on the interfaces (oil-water and air-water). The phenomenon could be related with depletion flocculation (Grundy et al., 2018). Indeed, the movements of particles and water probably decreased by increasing substitution, increasing the phase separation.

3.3.6. Storage stability

By reducing oil amount to 75%, an increase in droplet size was observed (Table 3 and Fig. 9). But more substitution to 100% decreased the average droplet size since water-oil interface was omitted, conjugates were only to be adsorbed on water-air interfaces. It was reported that increasing hydrocolloids concentration (xanthan, guar, and corn starch) reduced the droplet size as viscosity improved (Rahmati et al., 2015). Predictably, droplet size slightly increased during time. Interestingly, the droplets of S-75% and S-100% became more uniform after 14 days, showing that conjugates needed time for surface adsorption. It was proved that Maillard conjugates show desirable surface activity which improve the emulsion capacity and stability. The conjugation increases the β-sheets and random coils, resulting in more exposed hydrophobic groups. Besides, the steric stabilization facilitates adsorption of conjugates (Choi et al., 2023; Ouraji et al., 2020). It could be postulated that a thick viscoelastic layer of protein and polysaccharide formed in the interfaces of water-oil and water-air over time, which prevented flocculation of oil droplets and air bubbles.

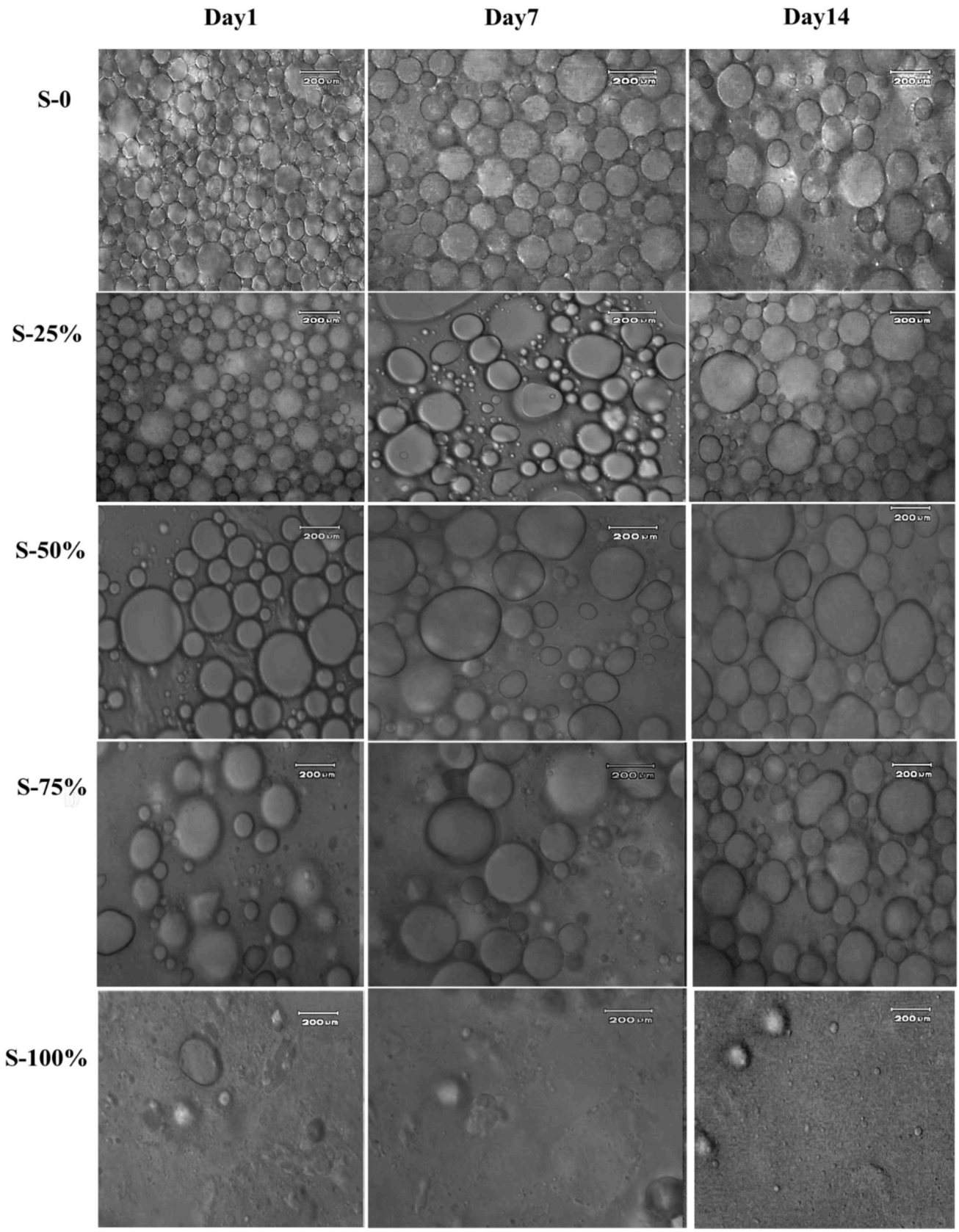

Fig. 9. The optical microscope images of mayonnaise samples during storage.

Table 3
The effect of substitution percentage on storage stability of mayonnaise samples.

Treatments	Thermal stability (%)	Average droplet size (μm)		
	Day 1	Day 1	Day 7	Day 14
S-0%	60.01^{gh}	162.44^{l}	362.61^{k}	438.29^{j}
S-25%	83.45^{b}	574.27^{i}	687.65^{h}	841.41^{g}
S-50%	89.65^{a}	1335.44^{c}	1542.96^{b}	1976.76^{a}
S-75%	93.18^{a}	1047.82^{e}	1280.61^{d}	996.46^{f}
S-100%	74.40^{cd}	52.60^{n}	81.59^{m}	62.37^{mn}

Means within the same column with different superscripts differ significantly ($P<0.05$).

3.3.7. Sensory properties

Samples with 25 and 50% substitution had lighter color ($P<0.05$) regarding the higher moisture content and better light scattering over control sample (Fig. 10). The textural sensory scores decreased by increasing substitution to 75 and 100% due to more air and water in the structure, while samples with up to 50% replacement had high textural scores besides showing desirable flavor and taste. So, homogeneous distribution of food components around taste buds and olfactory receptors made panellists finding the samples with up to 50% substitution desirable. However, higher replacement to 75 and 100% caused bitter and spicy flavor as oil reduced, so the tangy flavor of free vinegar was highlighted. Subsequently, lower hardness and cohesiveness made the sample less resistant toward flowing, so easy spreading of sample amplified the sensory perception (Bayarri et al., 2006). Furthermore, an increase in the moisture content could reduce the tongue-sample friction, facilitating in-mouth spreading of sample. It can, hence, be concluded that SPI-gellan gum conjugate aerated gel could be used in reduced fat mayonnaises since the overall acceptance increased up to 50% replacement. Similarly, microparticles of whey protein-pectin complex were successfully replaced in mayonnaise samples, and the low-calorie sauces with 20 and 40% replacement had a great overall acceptance (Sun et al., 2018).

4. Conclusions

This research aimed at designation and characterization of cold-set aerated gels based on SPI-gellan gum conjugates. Increasing heating time improved the textural and color properties, reduced density and WHC of aerated gels whereas the opposite trend was observed upon increasing protein concentration. Subsequently, conjugate produced in optimum conditions (1% gum, 1.5% SPI, and 90 min heating time) showed 35% glycation degree, and declined pH compared with non-conjugated sample. The SDS-PAGE pattern also showed that 7 S and 11 S bands became lighter and disappeared. All of which confirmed Maillard reaction.

Subsequently, the optimized aerated gel was produced with 300 mM $CaCl_2$ which was strain- and frequency-dependent, displaying a semi-elastic gel. In temperature sweep test, G' was greater than G", keeping the gel stable up to 90 °C. Moreover, an inhomogeneous surface but uniform microstructure was observed. The FTIR spectrum showed that the O-H stretching vibrations increased, confirming gelation and aeration. While the lower intensity of anomeric region of saccharides in optimized aerated gel spectrum represented Maillard reaction.

The optimized gel was eventually incorporated in mayonnaise sauce to produce a plant-based low-fat product, which improved the sauce nutritional value and thermal stability while the calorie significantly decreased. Thus, the aerated gel can be used as an oil substitute to improve the nutritional and physicochemical properties of food formulations.

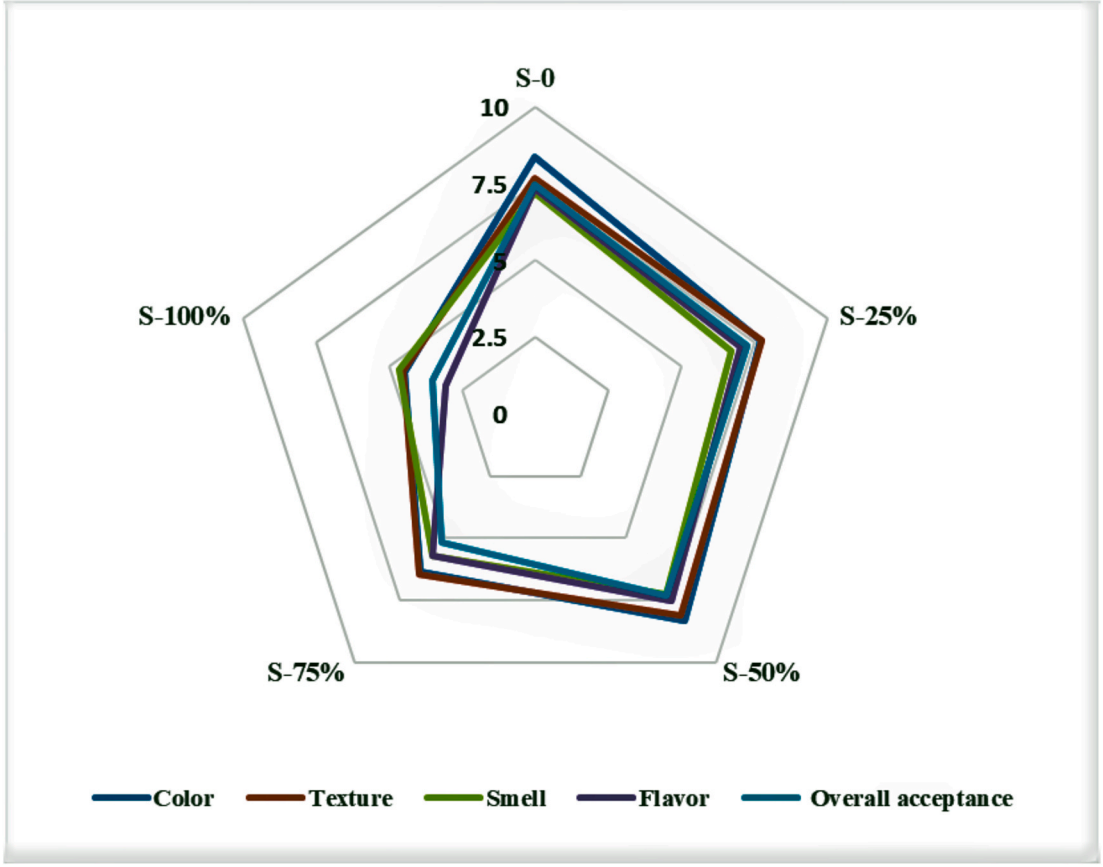

Fig. 10. Sensory spider chart for mayonnaise sauces.

CRediT authorship contribution statement

Setayesh Ferdowsian: Methodology, Formal analysis, Investigation, Writing – original draft, Resources, Software. **Zahra Kazemi-Taskooh:** Methodology, Validation, Writing – original draft, Writing – review & editing. **Mohammad Javad Varidi:** Supervision, Resources, Funding acquisition. **Majid Nooshkam:** Advisor, Methodology. **Mehdi Varidi:** Project administration, Supervision, Resources, Conceptualization, Methodology, Validation, Visualization.

Declaration of competing interest

The authors declare that they have no known competing financial interests or personal relationships that could have appeared to influence the work reported in this paper.

Acknowledgment

The authors would like to thank Ferdowsi University of Mashhad for the financial support (Grant Number 59515).

Appendix A. Supplementary data

Supplementary data to this article can be found online at https://doi.org/10.1016/j.crfs.2024.100923.

Data availability

Data will be made available on request.

References

Abaee, A., Mohammadian, M., Jafari, S.M., 2017. Whey and soy protein-based hydrogels and nano-hydrogels as bioactive delivery systems. Trends Food Sci. Technol. 70, 69–81. https://doi.org/10.1016/j.tifs.2017.10.011.

Ajandouz, E., Tchiakpe, L., Ore, F.D., Benajiba, A., Puigserver, A., 2001. Effects of pH on caramelization and Maillard reaction kinetics in fructose-lysine model systems. J. Food Sci. 66 (7), 926–931. https://doi.org/10.1111/j.1365-2621.2001.tb08213.x.

Al-Aubadi, I.M.K., 2021. Preparation of healthy mayonnaise by using plant and animal gums as oil replacer. Sys. Rev. Pharm. 12 (1), 1142–1150. https://doi.org/10.31838/srp.2021.1.157.

Alghooneh, A., Razavi, S.M., Kasapis, S., 2018. Hydrocolloid clustering based on their rheological properties. J. Texture Stud. 49 (6), 619–638. https://doi.org/10.1111/jtxs.12368.

Alkabaa, A.S., Akcicek, A., Taylan, O., Balubaid, M., Alamoudi, M., Gulzar, W.A., Alidrisi, H., Dertli, E., Karasu, S., 2024. Production of novel bigels from cold pressed chia seed oil by-product: application in low-fat mayonnaise. Foods 13 (4), 574. https://doi.org/10.3390/foods13040574.

Bayarri, S., Taylor, A.J., Hort, J., 2006. The role of fat in flavor perception: effect of partition and viscosity in model emulsions. J. Agric. Food Chem. 54 (23), 8862–8868. https://doi.org/10.1021/jf061537k.

Bi, C.-h., Zhu, Y.-d., Li, L.-t., Zhang, Y.-l., Hua, Z., Zhu, J.-y., Liu, Y., Liu, Y.-d., Huang, Z.-g., 2018. Rheological properties and microstructure of soy protein isolate/κ-carrageenan gels under high-speed shear treatment. J. Food Eng. 236, 44–50. https://doi.org/10.1016/j.jfoodeng.2018.05.006.

Boonlao, N., Ruktanonchai, U.R., Anal, A.K., 2023. Glycation of soy protein isolate with maltodextrin through Maillard reaction via dry and wet treatments and compare their techno-functional properties. Polym. Bull. 80 (8), 8603–8626. https://doi.org/10.1007/s00289-022-04473-y.

Chailangka, A., Seesuriyachan, P., Wangtueai, S., Ruksiriwanich, W., Jantanasakulwong, K., Rachtanapun, P., Sommano, S.R., Leksawasdi, N., Barba, F.J., Phimolsiripol, Y., 2022. Cricket protein conjugated with different degrees of polymerization saccharides by Maillard reaction as a novel functional ingredient. Food Chem. 395, 133594. https://doi.org/10.1016/j.foodchem.2022.133594.

Chen, W., Ma, X., Wang, W., Lv, R., Guo, M., Ding, T., Ye, X., Miao, S., Liu, D., 2019. Preparation of modified whey protein isolate with gum acacia by ultrasound maillard reaction. Food Hydrocolloids 95, 298–307. https://doi.org/10.1016/j.foodhyd.2018.10.030.

Choi, H.W., Ham, S.H., Hahn, J., Choi, Y.J., 2023. Developing plant-based mayonnaise using pea protein-xanthan gum conjugates: a maillard reaction approach. Lwt 185, 115137. https://doi.org/10.1016/j.lwt.2023.115137.

Damodaran, S., 2017. Food Proteins and Their Applications. CRC Press.

Dehghannya, J., Pourahmad, M., Ghanbarzadeh, B., Ghaffari, H., 2018. Influence of foam thickness on production of lime juice powder during foam-mat drying: experimental and numerical investigation. Powder Technol. 328, 470–484. https://doi.org/10.1016/j.powtec.2018.01.034.

Deng, B., De Ruiter, J., Schroën, K., 2019. Application of Microfluidics in the Production and analysis of food foams. Foods 8 (10), 476. https://doi.org/10.3390/foods8100476.

Derkach, S.R., Kuchina, Y.A., Kolotova, D.S., Voron'ko, N.G., 2020. Polyelectrolyte polysaccharide–gelatin complexes: rheology and structure. Polymers 12 (2), 266. https://doi.org/10.3390/foods8100476.

Dev, M.J., Pandit, A.B., Singhal, R.S., 2021. Ultrasound assisted vis-à-vis classical heating for the conjugation of whey protein isolate-gellan gum: process optimization, structural characterization and physico-functional evaluation. Innovat. Food Sci. Emerg. Technol. 72, 102724. https://doi.org/10.1016/j.ifset.2021.102724.

Gharachorloo, M., Yousefi, S., 2024. Optimization of oleogel production formulation based on sesame oil and its effect on physicochemical and quality properties of mayonnaise. J. Food Sci. Technol. 20 (144), 63–79. https://doi.org/10.22034/FSCT.20.144.63.

Ghasemi, B., Varidi, M.J., Varidi, M., Kazemi-Taskooh, Z., Emami, S.A., 2022. The effect of plant essential oils on physicochemical properties of chicken nuggets. J. Food Meas. Char. 1–12. https://doi.org/10.1007/s11694-021-01204-1.

Ghobadi, E., Varidi, M., Varidi, M.J., Koocheki, A., 2018. Fenugreek seed gum: extraction optimization and evaluation of antioxidant properties. Innov. Food Technol. 5 (3), 447–468. https://doi.org/10.22104/jift.2017.2173.1499.

Gökmen, V., Şenyuva, H.Z., 2007. Acrylamide formation is prevented by divalent cations during the Maillard reaction. Food Chem. 103 (1), 196–203. https://doi.org/10.1016/j.foodchem.2006.08.011.

Grundy, M.M., McClements, D.J., Ballance, S., Wilde, P.J., 2018. Influence of oat components on lipid digestion using an in vitro model: impact of viscosity and depletion flocculation mechanism. Food Hydrocolloids 83, 253–264. https://doi.org/10.1016/j.foodhyd.2018.05.018.

Herremans, E., Bongaers, E., Estrade, P., Gondek, E., Hertog, M., Jakubczyk, E., Nguyen Do Trong, N., Rizzolo, A., Saeys, W., Spinelli, L., Torricelli, A., Vanoli, M., Verboven, P., Nicolaï, B., 2013. Microstructure–texture relationships of aerated sugar gels: novel measurement techniques for analysis and control. Innovat. Food Sci. Emerg. Technol. 18, 202–211. https://doi.org/10.1016/j.ifset.2013.02.003.

Heydari, A., Razavi, S.M.A., 2021. Evaluating high pressure-treated corn and waxy corn starches as novel fat replacers in model low-fat O/W emulsions: a physical and rheological study. Int. J. Biol. Macromol. 184, 393–404. https://doi.org/10.1016/j.ijbiomac.2021.06.052.

Himashree, P., Sengar, A.S., Sunil, C., 2022. Food thickening agents: sources, chemistry, properties and applications-A review. Int. J. Gastron. Food Sci. 27, 100468. https://doi.org/10.1016/j.ijgfs.2022.100468.

Huang, Z.-g., Wang, X.-y., Zhang, J.-y., Liu, Y., Zhou, T., Chi, S.-y., Gao, F., Li, J., Tian, B., Shi, W.-t., Bi, C.-h., 2022. Effect of heat treatment on the nonlinear rheological properties of acid-induced soy protein isolate gels modified by high-pressure homogenization. Lwt 157, 113094. https://doi.org/10.1016/j.lwt.2022.113094.

Hyun, K., Kim, S.H., Ahn, K.H., Lee, S.J., 2002. Large amplitude oscillatory shear as a way to classify the complex fluids. J. Non-Newtonian Fluid Mech. 107 (1–3), 51–65. https://doi.org/10.1016/S0377-0257(02)00141-6.

Jakubczyk, E., Kamińska-Dwórznicka, A., 2021. Effect of addition of chokeberry juice concentrate and foaming agent on the physical properties of agar gel. Gels 7, 137. https://doi.org/10.3390/gels7030137.

Karunadasa, K.S., Manoratne, C., Pitawala, H., Rajapakse, R., 2018. Relative stability of hydrated/anhydrous products of calcium chloride during complete dehydration as examined by high-temperature X-ray powder diffraction. J. Phys. Chem. Solid. 120, 167–172. https://doi.org/10.1016/j.jpcs.2018.04.034.

Kazemi-Taskooh, Z., Varidi, M., 2021. Designation and characterization of cold-set whey protein-gellan gum hydrogel for iron entrapment. Food Hydrocolloids 111, 106205. https://doi.org/10.1016/j.foodhyd.2020.106205.

Kazemi-Taskooh, Z., Varidi, M., 2023. How can plant-based protein–polysaccharide interactions affect the properties of binary hydrogels?(A review). Food Funct. https://doi.org/10.1039/D3FO00611E.

Kazemi-Taskooh, Z., Varidi, M., 2024. Interaction-induced characterization of animal-based protein-polysaccharide composite hydrogels: a review. Food Rev. Int. 1–33. https://doi.org/10.1080/87559129.2024.2366857.

Ke, C., Li, L., 2023. Influence mechanism of polysaccharides induced Maillard reaction on plant proteins structure and functional properties: a review. Carbohydr. Polym. 302, 120430. https://doi.org/10.1016/j.carbpol.2022.120430.

Kuhn, K.R., Cavallieri, Â.L.F., Da Cunha, R.L., 2010. Cold-set whey protein gels induced by calcium or sodium salt addition. Int. J. Food Sci. Technol. 45 (2), 348–357. https://doi.org/10.1111/j.1365-2621.2009.02145.x.

Lavaei, Y., Varidi, M., Nooshkam, M., 2022. Gellan gum conjugation with soy protein via Maillard-driven molecular interactions and subsequent clustering lead to conjugates with tuned technological functionality. Food Chem. X 15, 100408. https://doi.org/10.1016/j.fochx.2022.100408.

Lee, M.-Y., Jo, Y.-J., 2023. Microstructural and rheological properties of heat-induced gels from mung bean protein aggregates. J. Food Meas. Char. 1–9. https://doi.org/10.1007/s11694-023-01898-5.

Li, J., Wang, Y., Jin, W., Zhou, B., Li, B., 2014. Application of micronized konjac gel for fat analogue in mayonnaise. Food Hydrocolloids 35, 375–382. https://doi.org/10.1016/j.foodhyd.2013.06.010.

Li, R., Cheng, Y., Tang, N., Wu, L., Nirasawa, S., Jia, X., Cao, W., 2020. Rheological, structural and physicochemical characteristics of heat-induced egg albumin/sesbania gum mixed gels. Int. J. Biol. Macromol. 163, 87–95. https://doi.org/10.1016/j.foodhyd.2013.06.010.

Li, J., Yang, X., Swallah, M.S., Fu, H., Ji, L., Meng, X., Yu, H., Lyu, B., 2022. Soy protein isolate: An overview on foaming properties and air–liquid interface. Int. J. Food Sci. Technol. 57 (1), 188–200. https://doi.org/10.1111/ijfs.15390.

Li, W., Zhao, H., He, Z., Zeng, M., Qin, F., Chen, J., 2016. Modification of soy protein hydrolysates by Maillard reaction: effects of carbohydrate chain length on structural and interfacial properties. Colloids Surf. B Biointerfaces 138, 70–77. https://doi.org/10.1016/j.colsurfb.2015.11.038.

Ma, X., Chen, W., Yan, T., Wang, D., Hou, F., Miao, S., Liu, D., 2020. Comparison of citrus pectin and apple pectin in conjugation with soy protein isolate (SPI) under controlled dry-heating conditions. Food Chem. 309, 125501. https://doi.org/10.1016/j.foodchem.2019.125501.

Ma, X., Chi, C., Pu, Y., Miao, S., Liu, D., 2022. Conjugation of soy protein isolate (SPI) with pectin: effects of structural modification of the grafting polysaccharide. Food Chem. 387, 132876. https://doi.org/10.1016/j.foodchem.2022.132876.

Ma, Y., Zhao, Y., Chi, Y., 2019. Changes in the gel characteristics of two hen egg white powders modified by dry heating and the Maillard reaction during long-term storage. Lwt 109, 123–129. https://doi.org/10.1016/j.lwt.2019.04.003.

Maltais, A., Remondetto, G.E., Gonzalez, R., Subirade, M., 2005. Formation of soy protein isolate cold-set gels: protein and salt effects. J. Food Sci. 70 (1), C67–C73. https://doi.org/10.1111/j.1365-2621.2005.tb09023.x.

Maltais, A., Remondetto, G.E., Subirade, M., 2008. Mechanisms involved in the formation and structure of soya protein cold-set gels: a molecular and supramolecular investigation. Food Hydrocolloids 22 (4), 550–559. https://doi.org/10.1016/j.foodhyd.2007.01.026.

Mandala, I., Savvas, T., Kostaropoulos, A., 2004. Xanthan and locust bean gum influence on the rheology and structure of a white model-sauce. J. Food Eng. 64 (3), 335–342. https://doi.org/10.1016/j.jfoodeng.2003.10.018.

Meydani, B., Vahedifar, A., Askari, G., Madadlou, A., 2019. Influence of the Maillard reaction on the properties of cold-set whey protein and maltodextrin binary gels. Int. Dairy J. 90, 79–87. https://doi.org/10.1016/j.idairyj.2018.11.009.

Miao, L., Zhu, J., Peng, X., Feng, J., Dong, H., Tong, X., Wang, H., Jiang, L., 2023. Effects of $CaCl_2$ concentration on fibrils formation and characteristics of soybean protein isolate and β-conglycinin/glycinin. Food Hydrocolloids 142, 108769. https://doi.org/10.1016/j.foodhyd.2023.108769.

Nikzade, V., Tehrani, M.M., Saadatmand-Tarzjan, M., 2012. Optimization of low-cholesterol–low-fat mayonnaise formulation: effect of using soy milk and some stabilizer by a mixture design approach. Food Hydrocolloids 28 (2), 344–352. https://doi.org/10.1016/j.foodhyd.2011.12.023.

Nooshkam, M., Madadlou, A., 2016a. Maillard conjugation of lactulose with potentially bioactive peptides. Food Chem. 192, 831–836. https://doi.org/10.1016/j.foodchem.2015.07.094.

Nooshkam, M., Madadlou, A., 2016b. Microwave-assisted isomerisation of lactose to lactulose and Maillard conjugation of lactulose and lactose with whey proteins and peptides. Food Chem. 200, 1–9. https://doi.org/10.1016/j.foodchem.2015.07.094.

Nooshkam, M., Varidi, M., Verma, D.K., 2020. Functional and biological properties of Maillard conjugates and their potential application in medical and food: a review. Food Res. Int. 131, 109003. https://doi.org/10.1016/j.foodres.2020.109003.

Ouraji, M., Alimi, M., Motamedzadegan, A., Shokoohi, S., 2020. Faba bean protein in reduced fat/cholesterol mayonnaise: extraction and physico-chemical modification process. J. Food Sci. Technol. 57, 1774–1785. https://doi.org/10.1007/s13197-019-04211-9.

Park, J.J., Olawuyi, I.F., Lee, W.Y., 2020. Characteristics of low-fat mayonnaise using different modified arrowroot starches as fat replacer. Int. J. Biol. Macromol. 153, 215–223. https://doi.org/10.1016/j.ijbiomac.2020.02.331.

Patole, S., Cheng, L., Yang, Z., 2022. Impact of incorporations of various polysaccharides on rheological and microstructural characteristics of heat-induced quinoa protein isolate gels. Food Biophys. 17 (3), 314–323. https://doi.org/10.1007/s11483-022-09720-3.

Peng, Z., Zhang, Y., Wang, H., Gao, G., Yu, Z., Chong, P.H., Ding, W., Ke, L., Zhou, J., Rao, P., 2021. Effects of arginine-glucose Maillard reaction products on the physicochemical and gel properties of chicken myofibrillar protein. Lwt 152, 112244. https://doi.org/10.1016/j.lwt.2021.112244.

Petcharat, T., Benjakul, S., 2017. Effect of gellan and calcium chloride on properties of surimi gel with low and high setting phenomena. RSC Adv. 7, 52423–52434. https://doi.org/10.1039/C7RA10869A.

Pi, X., Liu, J., Sun, Y., Sun, X., Sun, Z., Cheng, J., Guo, M., 2023. Investigation of the differences in the effect of (−)-epigallocatechin gallate and proanthocyanidins on the functionality and allergenicity of soybean protein isolate. Food Chemistry X 17, 100566. https://doi.org/10.1016/j.fochx.2023.100566.

Pourramezan, H., Labbafi, M., Khodaiyan, F., Mousavi, M., Gharaghani, M., Saadatvand, M., Mahmoudi, A., 2022. Preparation of octenyl succinylated kappa-carrageenan; reaction optimization, characterization, and application in low-fat vegan mayonnaise. Int. J. Biol. Macromol. 223, 882–898. https://doi.org/10.1016/j.ijbiomac.2022.10.218.

Rahmati, N.F., Mazaheri Tehrani, M., Daneshvar, K., Koocheki, A., 2015. Influence of selected gums and pregelatinized corn starch on reduced fat mayonnaise: modeling of properties by central composite design. Food Biophys. 10, 39–50. https://doi.org/10.1007/s11483-014-9356-1.

Sánchez, C.C., Patino, J.M.R., 2005. Interfacial, foaming and emulsifying characteristics of sodium caseinate as influenced by protein concentration in solution. Food Hydrocolloids 19 (3), 407–416. https://doi.org/10.1016/j.foodhyd.2004.10.007.

Sheng, L., Tang, G., Wang, Q., Zou, J., Ma, M., Huang, X., 2020. Molecular characteristics and foaming properties of ovalbumin-pullulan conjugates through the Maillard reaction. Food Hydrocolloids 100, 105384. https://doi.org/10.1016/j.foodhyd.2019.105384.

Spotti, M.J., Loyeau, P.A., Marangón, A., Noir, H., Rubiolo, A.C., Carrara, C.R., 2019. Influence of Maillard reaction extent on acid induced gels of whey proteins and dextrans. Food Hydrocolloids 91, 224–231. https://doi.org/10.1016/j.foodhyd.2019.01.020.

Sun, C., Liu, R., Liang, B., Wu, T., Sui, W., Zhang, M., 2018. Microparticulated whey protein-pectin complex: a texture-controllable gel for low-fat mayonnaise. Food Res. Int. 108, 151–160. https://doi.org/10.1016/j.foodres.2018.01.036.

Sun, M., Wang, C., Wang, H., Tan, M., 2025. Fish oil-based bigels with outstanding sensory and antioxidant properties: application in low-fat mayonnaise. Food Hydrocolloids 159, 110673. https://doi.org/10.1016/j.foodhyd.2024.110673.

Tomczyńska-Mleko, M., Mleko, S., Terpiłowski, K., Peréz-Huertas, S., Nishinari, K., 2022. Aerated whey protein gels as a controlled release system of creatine investigated in an artificial stomach. Innovat. Food Sci. Emerg. Technol. 79, 103060. https://doi.org/10.1016/j.ifset.2022.103060.

Totosaus, A., Montejano, J.G., Salazar, J.A., Guerrero, I., 2002. A review of physical and chemical protein-gel induction. Int. J. Food Sci. Technol. 37 (6), 589–601. https://doi.org/10.1046/j.1365-2621.2002.00623.x.

Vilela, J.A.P., Cavallieri, Â.L.F., Da Cunha, R.L., 2011. The influence of gelation rate on the physical properties/structure of salt-induced gels of soy protein isolate–gellan gum. Food Hydrocolloids 25 (7), 1710–1718. https://doi.org/10.1016/j.foodhyd.2011.03.012.

Villanueva, M., De Lamo, B., Harasym, J., Ronda, F., 2018. Microwave radiation and protein addition modulate hydration, pasting and gel rheological characteristics of rice and potato starches. Carbohydr. Polym. 201, 374–381. https://doi.org/10.1016/j.carbpol.2018.08.052.

Wang, W., Hu, C., Sun, H., Zhao, J., Xu, C., Ma, Y., Ma, J., Jiang, L., Hou, J., 2022. Physicochemical properties, stability and texture of soybean-oil-body-substituted low-fat mayonnaise: effects of thickeners and storage temperatures. Foods 11 (15), 2201. https://doi.org/10.3390/foods11152201.

Wang, X., He, Z., Zeng, M., Qin, F., Adhikari, B., Chen, J., 2017. Effects of the size and content of protein aggregates on the rheological and structural properties of soy protein isolate emulsion gels induced by CaSO4. Food Chem. 221, 130–138. https://doi.org/10.1016/j.foodhyd.2020.106205.

Wen-qiong, W., Pei-pei, Y., Ji-yang, Z., Zhi-hang, G., 2021. Effect of temperature and pH on the gelation, rheology, texture, and structural properties of whey protein and sugar gels based on Maillard reaction. J. Food Sci. 86 (4), 1228–1242. https://doi.org/10.1111/1750-3841.15659.

Xia, Z., Yao, X., Liu, W., Li, L., Kang, D., Yan, C., 2023. Effects of conjugates of ε-polylysine-dextran created through Maillard reaction on quality and storage stability of the chicken gel. Food Res. Int. 164, 112360. https://doi.org/10.1016/j.foodres.2022.112360.

Xiao, Y., Kang, S., Liu, Y., Guo, X., Li, M., Xu, H., 2021. Effect and mechanism of calcium ions on the gelation properties of cellulose nanocrystals-whey protein isolate composite gels. Food Hydrocolloids 111, 106401. https://doi.org/10.1016/j.foodhyd.2020.106401.

Yang, X., Gong, T., Lu, Y.-h., Li, A., Sun, L., Guo, Y., 2020a. Compatibility of sodium alginate and konjac glucomannan and their applications in fabricating low-fat mayonnaise-like emulsion gels. Carbohydr. Polym. 229, 115468. https://doi.org/10.1016/j.carbpol.2019.115468.

Yang, X., Li, A., Li, D., Guo, Y., Sun, L., 2021. Applications of mixed polysaccharide-protein systems in fabricating multi-structures of binary food gels—a review. Trends Food Sci. Technol. 109, 197–210. https://doi.org/10.1016/j.carbpol.2019.115468.

Yang, Y., Wang, Q., Lei, L., Li, F., Zhao, J., Zhang, Y., Li, L., Wang, Q., Ming, J., 2020b. Molecular interaction of soybean glycinin and β-conglycinin with (−)-epigallocatechin gallate induced by pH changes. Food Hydrocolloids 108, 106010. https://doi.org/10.1016/j.tifs.2021.01.002.

Yu, B., Ren, F., Zhao, H., Cui, B., Liu, P., 2020. Effects of native starch and modified starches on the textural, rheological and microstructural characteristics of soybean protein gel. Int. J. Biol. Macromol. 142, 237–243. https://doi.org/10.1016/j.foodhyd.2020.106205.

Zhang, X., Wang, Y., Li, Z., Li, Y., Qi, B., 2024. Effects of polysaccharide type on the structure, interface behavior, and foam properties of soybean protein isolate hydrolysate-polysaccharide Maillard conjugates. Food Hydrocolloids 151, 109801. https://doi.org/10.1016/j.foodhyd.2024.109801.

Zhao, C., Yin, H., Yan, J., Niu, X., Qi, B., Liu, J., 2021. Structure and acid-induced gelation properties of soy protein isolate–maltodextrin glycation conjugates with ultrasonic pretreatment. Food Hydrocolloids 112, 106278. https://doi.org/10.1016/j.foodhyd.2020.106278.

Zheng, S., Wei, F., Zheng, Q., Xiao, J., Cao, Y., Lan, Y., 2023. Fabrication of rice bran protein-sodium alginate-calcium double cross-linked foam template for oleogel preparation. Food Hydrocolloids 143, 108873. https://doi.org/10.1016/j.foodhyd.2023.108873.

Zúñiga, R., Aguilera, J., 2008. Aerated food gels: fabrication and potential applications. Trends Food Sci. Technol. 19 (4), 176–187. https://doi.org/10.1016/j.tifs.2007.11.012.